The underwater soundscape of the North Sea

F. Basan [a,*], J.-G. Fischer [a], R. Putland [b], J. Brinkkemper [c], C.A.F. de Jong [d], B. Binnerts [d], A. Norro [e], D. Kühnel [a], L.-A. Ødegaard [f], M. Andersson [g], E. Lalander [g], J. Tougaard [h], E.T. Griffiths [h], M. Kosecka [i], E. Edwards [i], N.D. Merchant [b], K. de Jong [j], S. Robinson [k], L. Wang [k], N. Kinneging [l]

[a] Federal Maritime and Hydrographic Agency (BSH), Germany
[b] Centre for Environment, Fisheries & Aquaculture Science (CEFAS), United Kingdom
[c] WaterProof Marine Consultancy & Services B.V., Netherlands
[d] Netherlands Organization for Applied Scientific Research (TNO), Netherlands
[e] Royal Belgian Institute of Natural Sciences (RBINS), Belgium
[f] Norwegian Defence Research Establishment (FFI), Norway
[g] Swedish Defence Research Agency (FOI), Sweden
[h] Aarhus University (AU), Department of Ecoscience, Denmark
[i] Marine Scotland (MS), United Kingdom
[j] Institute of Marine Research (IMR), Norway
[k] National Physical Laboratory (NPL), United Kingdom
[l] Rijkswaterstaat (RWS), Netherlands

ARTICLE INFO

ABSTRACT

As awareness on the impact of anthropogenic underwater noise on marine life grows, underwater noise measurement programs are needed to determine the current status of marine areas and monitor long-term trends. The Joint Monitoring Programme for Ambient Noise in the North Sea (JOMOPANS) collaborative project was funded by the EU Interreg to collect a unique dataset of underwater noise levels at 19 sites across the North Sea, spanning many different countries and covering the period from 2019 to 2020. The ambient noise from this dataset has been characterised and compared - setting a benchmark for future measurements in the North Sea area. By identifying clusters with similar sound characteristics in three broadband frequency bands (25–160 Hz, 0.2–1.6 kHz, and 2–10 kHz), geographical areas that are similarly affected by sound have been identified. The measured underwater sound levels show a persistent and spatially uniform correlation with wind speed at high frequencies (above 1 kHz) and a correlation with the distance from ships at mid and high frequencies (between 40 Hz and 4 kHz). Correlation with ocean current velocity at low frequencies (up to 200 Hz), which are susceptible to nonacoustic contamination by flow noise, was also evaluated. These correlations were evaluated and simplified linear scaling laws for wind and current speeds were derived. The presented dataset provides a baseline for underwater noise measurements in the North Sea and shows that spatial variability of the dominant sound sources must be considered to predict the impact of noise reduction measures.

1. Introduction

The North Sea is one of the busiest maritime areas in the world, therefore it is particularly affected by the environmental impacts associated with exploiting the oceans for transport and energy extraction. Unintended by-products of shipping, including air pollution and underwater radiated noise (URN), raise concerns for conservation and resource management. Along with the dilemma of the greenhouse gas emissions (e.g. Van Roy et al., 2022; Tattini and McBain, 2021; Wang et al., 2021; Olmer et al., 2017), the emission of underwater noise and the associated adverse effects on the marine environment are widely recognized. As the number of ships operating on the world's oceans increases, so does concern about the effects of ship noise on aquatic life (Hildebrand, 2009; Frisk, 2012; Ainslie et al., 2021).

Research studies in recent decades have shown that shipping noise can affect the behaviour and physiology of sensitive species of marine

---

* Corresponding author.
  E-mail address: fritjof.basan@bsh.de (F. Basan).

fauna, including marine mammals, fish and invertebrates (e.g. Richardson et al., 1995; Wisniewska et al., 2018; Thomsen et al., 2020; Duarte et al., 2021; Frankish et al., 2023). It is therefore essential to assess the impact of URN on the marine environment to evaluate future measures that can be taken to reduce the emission of URN.

In 2008, the Marine Strategy Framework Directive (MSFD) of the European Union (EU) recognized underwater noise as one of eleven descriptors that determine the environmental status of marine regions. Initially aiming to achieve or maintain a Good Environmental Status (GES) of the European Seas by 2020, all Member States were required to develop strategies or measures to achieve this status (European Commission, 2008). Those marine strategies also include monitoring and assessment of each descriptor that should be established to determine the state of all marine waters on a regular basis (Dekeling et al., 2014). The MSFD Technical Group on Underwater Noise (TG Noise) along with the OSPAR convention require the combined use of measurements and numerical models to determine levels and trends of ambient noise and encourage international collaboration within sub regions to guarantee consistent monitoring (Dekeling et al., 2014; Van der Graaf et al., 2012; Snoek et al., 2015). Such collaboration has been established for all European seas within the past decade in the form of regional projects (Merchant et al., 2022).

The EU project "Joint Monitoring Programme for Ambient Noise in the North Sea" (JOMOPANS), commissioned by the EU Interreg North Sea Region programme in 2018, was one of these projects. It aimed at developing a framework for joint monitoring of ambient noise to aid policy makers in evaluating the status of the North Sea in relation to URN. Data from 19 stations across the North Sea (Fig. 1) throughout the years 2019 and 2020 were shared between twelve institutions (NL[1,2,3] SE,[4] DK,[5] DE,[6] UK[7,8,9] BE,[10] NO[11,12]) to address the transnational issue of continuous underwater noise pollution in the North Sea region. The primary aim of the project was to -produce maps of ambient sound in the North Sea (taking into account shipping and wind as sound sources), from which URN was then assessed and coordinated measures developed (Kinneging et al., 2021).

The monthly statistical noise maps were produced for 2019 and 2020 by using models. These maps were validated with the in-situ measurements to assess the performance of the acoustic model (Putland et al., 2022). The modelled sound maps showed that shipping noise dominates the lower frequencies (up to 2 kHz) of the North Sea underwater ambient noise (de Jong et al., 2022). In southern parts and along major shipping lanes, the shipping noise exceeds the broadband natural sound of wind by >20 dB for >50 % of the time (Kinneging et al., 2023).

To enable policy makers to assess the impacts of URN, the JOMOPANS project further developed a management tool, in which the sound maps can be overlaid with distribution maps of sensitive species (Jomopans-Interreg North Sea Region, 2021).

Highlighting the model results of the JOMOPANS project we present the Dominance Noise Map for the whole year 2019 (Fig. 1), representing the areas of the North Sea that are mainly impacted by anthropogenic noise. The map shows over which percentage of the time anthropogenic noise dominates over the natural ambient noise by >20 dB (in the

broadband frequency range from 10 Hz to 20 kHz).

Most stations are located in the relatively shallow waters of the North Sea (below 50 m) - only the Scottish and Norwegian stations are in deeper waters (max. 340 m at the 13-NO-LOV station). The relatively shallow depths in the North Sea are an important feature for the sound propagation in the area. The depths determine the dominant frequency that propagates through the water (Jensen and Kuper, 1983) and due to the shallow depths; propagation loss with range is greater compared to deeper waters (see Table 2 and Fig. A for depths at the measurement stations and an overview of the bathymetry in the North Sea). For more context and further orientation maps of the three main variables treated in this study (currents, wind and shipping) are provided in the supplementary material (see supplementary Figs. B-D).

For the North Sea region, the JOMOPANS measurements are unique in terms of international collaboration, the number of stations, their spatial extent and the extended time period over which data are available. However, similar large-scale monitoring efforts have preceded JOMOPANS in other regions – e.g. the BIAS project in the Baltic Sea (Mustonen et al., 2019) and the national monitoring of the United States (Haver et al., 2018).

The measurements provide an opportunity to evaluate the overall ambient noise and not only quantify sounds from specific animals or specific anthropogenic activities, which is often the aim of passive acoustic monitoring. In this study, the overall objective was to explore the collected measurement data in more detail to answer the following three questions:

1. What are the acoustic characteristics at the individual stations and what are similarities across the stations?
2. Which frequency bands are affected by, and how are sound pressure levels related to, wind and shipping?
3. What is the impact of flow noise on the measurement data?

Wind-generated sound is the predominant natural component of the marine underwater ambient soundscape (Knudsen et al., 1948; Wenz, 1962). Waves are created and grow by the wind blowing over the water surface. During periods of higher wind speeds, waves break and create sound underwater by oscillation of bubbles from entrained air (Banner and Cato, 1988; Medwin and Beaky, 1989). Between 500 Hz and 50 kHz, wind-generated sound often dominates, depending on the location, water depth, wind conditions and the presence of other sound sources (see Fig. 3 as an example). In accordance with the wind noise model that was used in JOMOPANS (de Jong et al., 2021) a clear correlation and a linear scaling is expected between logarithmic wind speeds and measured acoustic sound levels (Ainslie, 2010; de Jong et al., 2022; Hildebrand et al., 2021). Importantly, as the prevailing wind and sea state conditions are closely connected, the wind field may indirectly influence other sound sources (e.g. decrease in ship traffic or offshore activities due to high sea state). Increased wind speed also affects the propagation of ship noise through increased attenuation and scattering when sound interacts with the rougher sea surface.

The significant energy of underwater sound emitted by vessels has often been described to be between 10 Hz and 1000 Hz (e.g. Richardson et al., 1995; Hildebrand, 2009; Merchant et al., 2012). However, Hermannsen et al. (2014) also showed considerable energy above ambient sound levels up to 150 kHz at distances to the ship between 60 and 1000 m. Small boats with proportionally smaller engines and faster revolving propellers generate less low frequency noise (Au and Green, 2000; Hermannsen et al., 2019), which is particularly relevant for more coastal stations such as 01-SE-VIN or 11-SC-HEL, where close passages of small boats are likely. Ships operating in DP (dynamic positioning) mode to stay at a certain position using bow and stern thrusters also emit sound in higher frequencies - up to 16 kHz (Fischer, 2000). This might affect measurements near offshore wind farms or oil rigs, such as 06-DE-FN1 or 18-DK-EDA where service vessels operate in DP-mode on a regular basis.

Flow of water around the surface of a hydrophone induces local

1. Rijkswaterstaat Ministerie van Infrastructuur en Waterstaat
2. Netherlands Organization for Applied Scientific Research (TNO)
3. WaterProof Marine Consultancy & Services B.V.
4. Swedish Defence Research Agency (FOI)
5. Department of Ecoscience - Aarhus Universitet
6. Federal Maritime and Hydrographic Agency (BSH)
7. Marine Scotland
8. National Physical Laboratory (NPL)
9. Centre for Environment, Fisheries and Aquaculture Science (CEFAS)
10. Royal Belgian Institute of Natural Science (RBINS)
11. Institute of Marine Research (IMR)
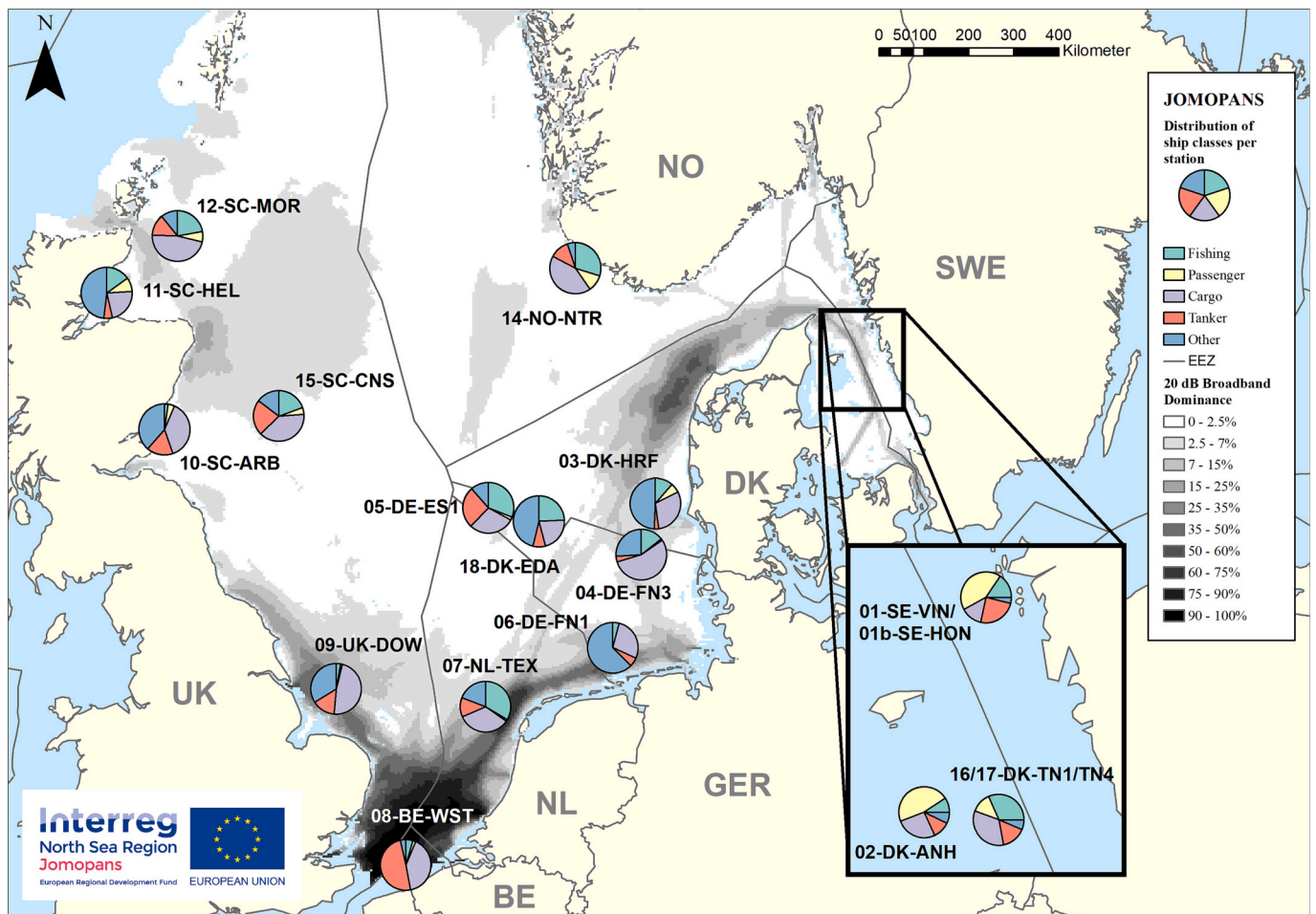12. Norwegian Defence Research Establishment (FFI)

Fig. 1. Positions of 18 measurement stations indicated by pie charts depicting the share of ship classes on total traffic within 35 km of each station; contour map in the background exhibits over what percentage of the year 2019 the predicted anthropogenic noise dominates the natural ambient noise by 20 dB or more (broadband 10 Hz - 20 kHz), underlying sound map adopted from (de Jong et al., 2022); note that the 13-NO-LOV station is not depicted in the figure as it is outside the modelled region; its coordinates are given in Table 2.

pressure fluctuations that result in low frequency signals in the measurements, called flow noise. Flow noise is not part of the ambient noise but is a contaminating low frequency signal in sound recordings. Currents can also induce noise in the measurements by for example causing vibration of the setup (e.g. cable strum), which is referred to as platform self-noise. The range of the turbulent pressure fluctuation covers the frequency range between 1 - ~100 Hz (cf. Robinson et al., 2014). Currently, there is no standard method to remove the effect of this noise from the measurements, but there are practicable approaches to describe it and exclude the contaminated data from the analysis (van Geel et al., 2020). This is particularly important when it comes to assessment (Borsani et al., 2023) and when validating numerical model results (Putland et al., 2022).

It is expected that at measuring stations with a strong tidal current regime, the flow-noise component would be clearly visible in the low frequency acoustic data (see Fig. 3). The current pattern of the North Sea is mainly dominated by tides (Sündermann and Pohlmann, 2011). However, the orbital motion of sea surface waves also creates currents that decrease with depth (e.g. Soulsby and Smallman, 1986). The depth to which orbital motion is still present equals roughly half the wavelength. With wave periods, ranging approximately from 6 to 8 s (Bonaduce et al., 2019), the average wavelength in the North Sea is expected to be between 56 m and 99 m (Holthuijsen, 2007). It is thus expected that orbital motion of wind driven waves can contribute to flow noise at stations in waters shallower than 50 m. Currents can further be forced geostrophically or can be caused by other phenomena

such as Langmuir circulation or Ekman spirals (e.g. Li et al., 2013; Sündermann and Pohlmann, 2011).

This study is structured as follows. First, the acoustic and environmental data are introduced. Second, similarities and differences between geographical positions are identified, and last correlations of sound levels with data on wind, shipping and currents are presented.

2. Data

For the presented analyses, acoustic and shipping data (AIS (Automatic Identification System) data purchased from the French company Quiet Oceans complemented by VMS (Vessel Monitoring System) data from Denmark, Germany, Norway and Sweden) from the JOMOPANS project, wind data from the E.U. Copernicus Marine Service, and ocean current data from the BSH operational hydrodynamic model, were used. These sources are elaborated in the Sections 2.1 to 2.4 below.

2.1. Acoustic data

Ambient sound was measured at 18 stations across the North Sea and at one reference station outside the North Sea at the Lofoten Islands (Fig. 1 and Table 2). The scope of the JOMOPANS project was limited to waters deeper than 10 m, thus all stations were located relatively far from the coast. Measurements were conducted in 8 different countries by representative partner organisations.

Depending on equipment availability, these partner organisations

elected to deploy either fixed cabled stations with real time data transfer and continuous power, or autonomous systems that had to be retrieved intermittently for data download (see Table 2). The measurement cycle varied between the stations, while some stations (mainly the cabled ones) were measuring continuously, most stations recorded using duty cycles (Fischer et al., 2021).

A variety of measurement systems were used (cf. Fischer et al., 2021), as project partners could choose which devices they preferred or already had available for the measurements. However, to ensure comparability between the measurements, the hardware used to record sound data had to meet technical standards set within the JOMOPANS project and had to be deployed 2–3 m above the seafloor (Fischer et al., 2021). Moreover, several quality assurance checks were performed on the data following the project's standards for data processing – i.e. checks for missing data and data consistency, removal of contaminated data (recordings before deployment, after recovery and during deployment, recovery and maintenance), checks for clipping, distortion and spurious signals – i.e. low frequency periodicities, periodic impulsive sounds and noise floor limitations (Ward et al., 2021).

Each partner ensured that the measured waveform data was converted to calibrated absolute power density spectra. The sound pressure level (SPL) was defined in the JOMOPANS Terminology Standard (Robinson and Wang, 2021) based on ISO 18405:2017 and represents the mean-square sound pressure averaged over a specified time, expressed as a level in decibels relative to a reference sound pressure value of 1 μPa. Data with averaging times (T) of 1 s or 20 s were shared among the project participants depending on the individual country's data policy.

Making use of Parseval's theorem the sound pressure level is given by:

$$L_p = 10 log_{10} \left(\frac{1}{N p_0^2} \sum_{k=1}^{N} |P_k|^2 \right)$$

where N is the number of samples within the averaged time T, p_0 is the reference sound pressure 1 μPa and P_k are the coefficients in the discrete Fourier transform (DFT) of the sound pressure time series. The sound pressure level in one-third octave frequency bands (base-10) (TOL) were obtained by calculating the power sum of the individual coefficients in the respective frequency band (Ward et al., 2021). These frequency bands are commonly used in acoustics (IEC 61260-1:2014) and are also termed "one-tenth decade" or "decidecade" bands (ISO 18405:2017). It was agreed to measure and share TOLs for the 34 one-third octave bands between 10 Hz and 20 kHz (Merchant et al., 2018).

The acoustic metrics (presented in Table 1) were chosen to be 1) realistic (in terms of practical constraints on monitoring), 2) ecologically relevant (reflect the way marine species are affected by sound) and 3) easily understood by non-specialists (Merchant et al., 2018).

To ensure a consistent application of the processing methods between measurement partners, a benchmark exercise was carried out where each partner processed synthetic noise signals generated with known statistics in a benchmark test of their own analysis routines. The test verified that, notwithstanding small variations between the partners' results (i.e. deviations of power averaged sound pressure levels below 1 dB), reported spectral density and power spectrum could be

Table 1
Summary of acoustic metrics.

Attribute	Specification
Physical quantity	Sound pressure level in dB re 1 μPa
Snapshot duration	1 s or 20 s
Analysis bandwidth	One-third octave (base 10)
Center frequencies	From 10 Hz to 20 kHz, defined according to the base-ten convention (ANSI, 2009; IEC 61260-1:2014)

processed consistently (Ward et al., 2021).

In total 4720 days of acoustic recordings were collected during the project lifetime at the 19 measurement stations (see Fig. 5). Gaps in the data coverage can in part be explained by the initial plan to only measure during the year 2019, although most countries continued measuring during 2020 as part of their national monitoring activities. Furthermore, some stations were not primarily JOMOPANS stations and therefore coverage was not expected to be complete. As such, data from the Swedish Vinga (01-SE-VIN) station, the two Norwegian stations (13-NO-LOV and 14-NO-NTR) and the Danish EDNA (18-DK-EDA) station are only available for the year 2019. Excluding data that did not pass the quality assurance checks described above further introduced gaps in the data coverage.

Considering the ambitious aim to measure at 19 stations for one year and the challenges associated with measuring at sea and during a pandemic (lost equipment, irregular maintenance intervals, operational difficulties for working at sea) the collected dataset during JOMOPANS is the largest of its kind and provides a remarkable and unique asset.

2.2. Wind data

Hourly modelled wind data for the entire study area were retrieved from the E.U. Copernicus Marine Service. These data were generated based on the ERA5 climate reanalysis, which is produced by the European Centre for Medium-Range Weather Forecasts (ECMWF) (Hersbach et al., 2018). The data were provided on a $0.25° \times 0.25°$ spatial grid and were subsequently interpolated to the respective positions of the JOMOPANS measurement stations (de Jong et al., 2021). The hourly amplitudes of the modelled wind speed were derived from the (zonal) U- and (meridional) V- components by:

$$v_{1h} = \sqrt{v_u^2 + v_v^2}$$

Annual mean wind speeds of the year 2019 at the individual stations are summarised in Table 2 and an overview map of mean wind speeds in the North Sea for 2019 is provided in Fig. B in the supplementary material.

2.3. Shipping data

To quantify the anthropogenic share of underwater noise related to vessel traffic, AIS data and VMS data were utilised as sources for the spatial distribution of ships in the North Sea. According to SOLAS requirements (International Convention for the Safety of Life at Sea) all ships of 300 or more gross tonnage (GT) and all passenger vessels must be fitted with an AIS system. Under European Union legislation fishing vessels exceeding 15 m are required to carry VMS transmitters in order to track and monitor fishing activities.

In JOMOPANS, processed AIS and VMS (provided by Denmark, Germany, Norway and Sweden) data for 2019 were acquired from the French company Quiet Oceans, which fused AIS and VMS data, cleaned outliers and duplicates, and interpolated the data onto a regular grid.

This merged dataset was further processed and checked for validity and consistency by TNO before it was used as input parameter for the sound maps of the North Sea that were also produced as part of the JOMOPANS project (de Jong et al., 2021). The correlations presented in this study, are based on the merged and processed dataset for the year 2019 as provided by TNO.

To give an overview of the average shipping density per acoustic measurement station, the number of vessels present within a 35 km radius (the estimated radius within which ships could be detected acoustically) during 15 min periods (as explained in Section 3.2.2) were summed over the year 2019 per station and referenced to the sum at the Belgian Westhinder station (08-BE-WST), where the most vessel passages were registered (Table 2). An overview of the shipping density in

Table 2

Summarised information on location, equipment and conditions at the measurement sites, "Shipping volume" describes the sum of unique vessels being within a 35 km radius throughout the year 2019 around each station for time steps of 15 min referenced to the 08-BE-WST station; 13-NO-LOV was located outside the modelled area for currents, wind and AIS; Measurement setups are given to be autonomous (a) or cabled (c).

Station	Position LAT | LON		Measurement setup	Shipping volume referenced to 08-BE-WST	Max. bottom current velocity [ms⁻¹]	Mean 10 m wind speed [ms⁻¹]	Water depth [m]	No. of measured days (2019 & 2020)
01-SE-VIN	57.623	11.572	c/a	70 %	0.16	6.67	45.0	316
01b-SE-HON	57.676	11.671	a	77 %	–	5.22	30.0	182
02-DK-ANH	56.927	11.200	a	21 %	0.21	7.50	12.0	200
03-DK-HRF	55.575	7.438	a	16 %	0.37	8.13	14.9	211
04-DE-FN3	55.195	7.158	c/a	13 %	0.23	8.17	21.8	204
05-DE-ES1	55.626	4.099	a	8 %	0.42	8.06	32.0	370
06-DE-FN1	54.015	6.588	c/a	44 %	0.56	7.95	33.9	362
07-NL-TEX	53.316	4.043	a	33 %	0.63	7.85	30.0	328
08-BE-WST	51.383	2.445	c/a	100 %	0.99	7.54	21.0	127
09-UK-DOW	53.529	1.053	a	27 %	0.44	7.29	21.0	633
10-SC-ARB	56.500	−2.380	a	8 %	0.23	6.66	48.0	347
11-SC-HEL	57.976	−3.536	a	6 %	0.10	6.78	50.0	286
12-SC-MOR	58.575	−2.120	a	9 %	0.31	8.10	80.0	104
13-NO-LOV	68.910	14.380	c	–	–	–	258.0	80
14-NO-NTR	58.237	5.839	a	23 %	0.12	8.30	340.0	332
15-SC-CNS	56.647	−0.094	a	3 %	0.32	7.97	81.0	66
16-DK-TN1	56.919	11.758	a	53 %	0.21	7.42	38.0	210
17-DK-TN4	56.902	11.6482	a	48 %	0.17	7.49	17.2	329
18-DK-EDA	55.474	5.110	a	20 %	0.25	8.10	45.0	33

the North Sea of 2019 is provided in Fig. C in the supplementary material.

2.4. Ocean current data

Ocean current velocity data were derived from the operational hydrodynamic model of BSH (Brüning et al., 2021). The layer closest to the seafloor was selected as all hydrophones were placed 2–3 m above the seafloor (cf. Fischer et al., 2021). The modelled currents were forced by wind, pressure gradients and tidal forces. The temporal resolution of the modelled data was 15 min and included data on current velocity and direction. The spatial resolution of the model was three nautical miles, and for each individual sound measurement station the output at the nearest grid point was selected. The maximum bottom current velocities per station are given in Table 2 and a map of bottom currents is shown Fig. D in the supplementary material.

3. Methods

3.1. Comparison of acoustic measurements

The available data and variability in the measured TOLs were visualised as spectrograms and Spectral Probability Density (SPD) plots. SPD plots comprehensively depict characteristics of ambient sound levels by presenting the empirical probability density of the measured TOLs. As proposed by Merchant et al. (2013) this presentation was combined with conventional percentiles and spectral averages. The

underlying distribution of sound levels was revealed, and outliers and multimodalities were detected.

Broadband sound pressure levels at the stations were compared quantitatively. The three chosen bands (D1, D2 and D3) resemble the decadal bands covering the frequencies in the 20 Hz - 160 Hz, 0.2 kHz - 1.6 kHz and 2 kHz to 16 kHz one-third octave bands. These frequency bands were also the focus of executed modelling during JOMOPANS, and broadly represent the hearing range of different animal groups (de Jong et al., 2022). To account for missing data at some stations, the low-frequency band (D1) only includes frequencies down to 25 Hz and the highest band (D3) only includes frequencies up to 10 kHz. Temporal variability in these frequency bands was examined using the 5th, 50th, and 95th percentile.

To quantitatively identify clusters, the broadband SPLs were compared pairwise using a two-sample Kolmogorov-Smirnov (KS) test (Smirnov, 1939). The Test Variable, as a convenient measure of similarity between distributions, gives a numerical indication on how similar the cumulative distribution functions of the respective broadband levels (D1-D3) were at all stations (ranging from 0 to 1, where 0 represents identity). The Kolmogorov-Smirnov statistic is given by:

$$D_{n,m} = sup|S_n(x) - S_m(x)|$$

where S_n and S_m are the cumulative distribution functions of broadband sound pressure level time series at two stations and *sup* is the supremum function.

The KS Test statistic provides an estimate on how similar the SPL distributions are in terms of location and shape (width and peak values).

A pairwise KS-test was conducted between all available data for all stations in all three bands. The hierarchical clustering technique was used to find similar stations in the resulting matrices of KS-test statistics. Pairs of stations (or groups of stations) with minimum Euclidean distance (classical method for distance measures) between their KS-test statistics were grouped together using the linkage function (*linkage* MATLAB version R2020b). The Euclidean distance (d_{euc}) is defined as:

$$d_{euc}(x, y) = \sqrt{\sum_{i=1}^{n}(x_i - y_i)^2},$$

where x and y are the two vectors of KS-test statistics of two stations and n is the total number of stations (Fig. 8). The closer d_{euc} between two stations is to 0, the more similar are the recorded sound pressure levels of these stations in the frequency band under consideration.

3.2. Correlation with wind, shipping and currents

To characterise the measured ambient noise at each station, correlations were calculated of all acoustic data from 2019 with wind speeds
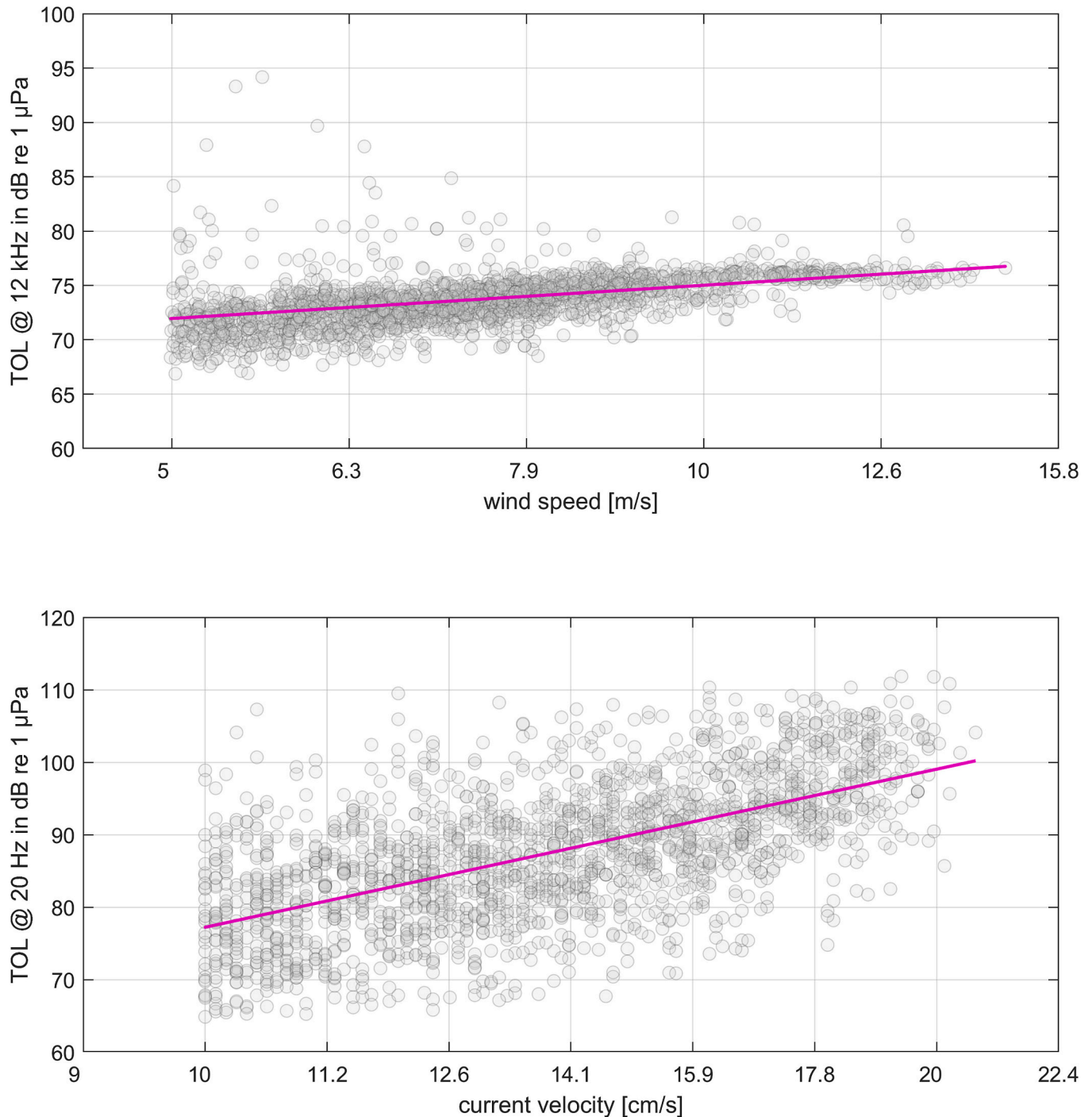

Fig. 2. Example of linear regressions between TOLs centred at different frequencies and: logarithmic wind speeds (top) and current velocities (bottom); slopes of regression lines (magenta) represent scaling law between TOLs and respective parameter; example data taken from Scottish 10-SC-ARB station; more examples for all stations are provided in Fig. E in the supplementary material. (For interpretation of the references to colour in this figure legend, the reader is referred to the web version of this article.)

at 10 m above the sea surface and range corrected point estimates of ships' contribution to ambient sound levels. TOLs were further correlated with bottom currents to evaluate the contaminating effect of flow noise on the measurements.

Since the averaging time (1 s or 20 s) and the duty cycles of the submitted acoustic data varied from partner to partner, simple correlations provided a straightforward method to distinguish the impact of these three parameters on the individual measurements.

To allow for the non-parametric distributions of the compared parameters, all presented correlation coefficients are Spearman Correlation Coefficients (Spearman, 1904).

Linear regressions allowed deriving a linear scaling law between the measured TOLs and wind speeds and current velocities (example in Fig. 2) for each station. These scaling laws allow for comparison with existing studies and provide a tool to estimate sound levels in areas without available measurements.

3.2.1. Wind induced sound component

The strength and direction of association between model-generated wind velocity and each TOL was measured using the non-parametric, Spearman correlation test.

As in Hildebrand et al. (2021) wind speeds below 5 m/s were neglected in the analysis. Modelled wind speed data were correlated with sound pressure levels for 17 project monitoring stations (the Norwegian station 13-NO-LOV and the Swedish 1b-SE-HON station were excluded as these stations were, respectively, not located in the area of interest or had no data available from 2019) to verify local wind-related ambient sound correlation at specific positions for different frequency bands. Wind noise at the Norwegian LoVe station has been studied by Ødegaard et al. (2019).

3.2.2. Shipping induced sound component

To quantify shipping density, a distance-weighted measure of vessels present is introduced and Spearman correlation coefficients are calculated with all TOLs.

Unique vessel presence within a 35 km radius around each station was determined in time steps of 15 min, including vessels 7 min before and after each time step. The basic assumption is that the received sound pressure level ($L_{p,i}$) for a ship is proportional to the logarithmic distance from a ship (Ainslee et al., 2014).

$$L_{p,i} = L_{S,i} - \left(A + B log_{10}\left(\frac{r_i}{r_0}\right)\right) dB, \text{ with } r_0 = 1 \text{ m}.$$

Where $L_{S,i}$ is the source level of a ship, A is the propagation constant, B is the transmission loss factor and r_i is the distance between the ith ship and the hydrophone. For each time step ($+/- 7$ min), the received sound pressure level at a hydrophone is thus proportional to the level sum of all $L_{p,i}$, i.e. the sum of all contributions from individual ships:

$$L_{p,\text{sum}} = 10 log_{10}\left(\sum_{i=1}^{N} 10^{\frac{L_{p,i}}{10 \text{ dB}}}\right) dB$$

In order to simplify the relationship between received sound pressure levels and vessels present we assume that source levels are the same for all ships and that the propagation constant A is also the same for all stations. The distance weighted metric for shipping CS (contributing shipping), is then given by:

$$CS = L_{p,\text{sum}} - L_S + A = 10 log_{10}\left(\sum_{i=1}^{N} 10^{-0.1 \ B log_{10}\left(\frac{r_i}{r_0}\right)}\right) dB$$

which reduces to:

$$CS = 10 log_{10}\left(\sum_{i=1}^{N} \left(\frac{r_i}{r_0}\right)^{-0.1 \ B}\right) dB$$

As B is not known around the stations and for all frequencies, and it

could be shown that the resulting correlation coefficients are not very sensitive to changes in B, it was decided to assume B to be 20 (transmission loss factor for spherical spreading and unit of propagation loss).

CS is thus a simplified index of the contribution from shipping to overall received sound levels. It is distance weighted and responsive to presence of multiple ships at different distances.

This simplified approach was found to be suitable for the intended analysis of identifying frequency bands correlated with shipping, but not for estimating the energy received from ships.

Linear scaling laws were found to be too simplistic and would not reflect the complex relationship between measured TOLs and shipping, which depends on many different factors.

Only vessels that were in direct line of sight of the hydrophone (i.e. not shadowed by land) and travelling at speeds above 0.1 knots were included. A time series of CS along with a spectrogram of a 5-day period is presented in Fig. 4.

3.2.3. Ocean current induced noise component (flow noise)

To identify frequency bands affected by flow noise, Spearman correlation coefficients of TOLs and modelled bottom current velocity were calculated.

Due to the highly variable current velocities across the stations no absolute lower cut-off velocity was defined (as was done in (van Geel et al., 2020)). Instead, to avoid periods of very low sound pressures, which can be close to the noise floor of the hydrophone, and to account for the uncertainty of the hydrodynamic model, only current velocities above the median current velocity per station were considered for correlations. An example of a regular flow noise pattern below 50 Hz, induced by tidal currents is shown in Fig. 3.

4. Results

4.1. Acoustical characteristics of JOMOPANS measurement stations

4.1.1. Spectrograms

The spectrograms, depicted in Fig. 5, show the temporal course of the TOLs at all JOMOPANS stations. Seasonal fluctuations appear to be negligible compared to the differences between stations, indicating high spatial variability in contrast to low temporal variability of the sound field in the North Sea.

Stations close to shipping lanes such as 06-DE-FN1, 07-NL-TEX, 08-BE-WST or 16-DK-TN1 show relatively high TOLs over large parts of the frequency range and during most of the time. The TOLs at the 09-UK-DOW station were further elevated due to construction noise at the Triton Knoll wind farm from January to August 2020, which is only 18 km away from the station. Although this posed by far the longest recorded period of construction noise in our dataset, other stations were also impacted by shorter periods of construction activities or seismic surveys (e.g. 05-DE-ES1 and 18-DK-EDA).

Lower TOLs were measured at 16-DK-TN1 following the rerouting of the major shipping lanes in the Kattegat from the 1st of July 2020. The data at the neighbouring 17-DK-TN4 does not show a clear change at this date. The associated effects of the rerouting are analysed in more detail in (Lalander et al., 2022).

The spectrograms show clearly that the deep Scottish and Norwegian stations (10-SC-ARB, 11-SC-HEL, 12-SC-MOR, 13-NO-LOV, 14-NO-NTR and 15-SC-CNS) were measuring relatively low TOLs compared to shallower, southern JOMOPANS stations (e.g. 06-DE-FN1, 07-NL-TEX, 08-BE-WST and 09-UK-DOW).

Surprisingly high TOLs were measured at station 05-DE-ES1 in the central part of the North Sea at the Doggerbank. Relatively low anthropogenic noise levels were expected at this station, given the remoteness from shipping lanes. Some stations were also affected constantly by tonal sounds (visible as horizontal lines throughout the spectrogram). At 03-DK-HRF and 04-DE-FN3 this can be linked to the mains hum of adjacent Offshore Wind installations.

Fig. 3. Bottom current velocities (top), wind speeds (middle) and spectrogram of measurements (bottom); lower frequencies (< 50 Hz) are distorted by tidal flow noise; two-weekly neap-and spring tide is visible, dominated by semi-diurnal tidal constituents; TOLs for frequencies above 1 kHz can be found to increase with higher wind speeds (example from August–October 2019 at location 07-NL-TEX);.

4.1.2. SPD

The spectral probability densities of all stations over the entire measurement period (2019–2020) are shown in Fig. 6. The grey scale indicates the probability density for each TOL, which gives the frequency of occurrence of acoustic conditions. The coloured lines indicate cumulative probability distributions of selected temporal percentiles (1 %, 5 %, 50 %, 90 % and 99 %).

This comprehensive overview depicts the diversity of recorded soundscapes. High variability across all frequencies can be seen at the stations in the Kattegat (16-DK-TN1 and 17-DK-TN4), in contrast to the deep 14-NO-LOV station or the 15-SC-CNS station for which TOLs have minimal variation. Variability at low frequencies was interpreted as an indicator for the regular influence of currents, which induced flow noise and/or platform self-noise, e.g. at the stations 01-SE-VIN, 02-DK-ANH, 03-DK-HRF, 06-DE-FN1, 07-NL-TEX, 08-BE-WST, 09-UK-DOW and 14-NO-NTR. Low frequency TOLs at the stations 05-DE-ES1 and 15-SC-CNS, which are both located near the amphidromic points of the North Sea, as well as recordings at the 13-NO-LOV station do not show these fluctuations related to tidal flow noise.

The SPDs reveal that the highest TOLs at all stations were recorded in the low to mid-frequency range between 100 Hz and 500 Hz, which is the typical frequency range for shipping noise and operational wind

farm noise. Lowest levels were recorded at the relatively deep (deeper than 48 m) Scottish and Norwegian stations (10-SC-ARB, 11-SC-HEL, 13-NO-LOV, 14-NO-NTR), but also at the Swedish 01b-SE-HON station in the Gothenburg archipelago (where the islands may provide acoustical shadows from the main shipping lane).

Notably there is high variability of lowest received TOLs across the stations. The lowest received levels do not only show the lowest ambient sound levels, but also reveal noise floor limitations of recording systems. Where probability densities converge with the cumulative probability distribution of the 1 % percentile the noise floor limits the measurement of natural ambient sound levels (e.g. at 05-DE-ES1 below 40 Hz or at 14-NO-NTR above 10 kHz).

SPD analysis also facilitated the detection of local peaks at specific frequencies. At 04-DE-FN3, a peak at 125 Hz was most likely caused by generator or platform noise. At 10-SC-ARB, the peak in RMS levels at 12 kHz was likely caused by the presence of marine mammals. The peak at 25 Hz in the 17-DK-TN4, cannot be linked to a specific sound source without further investigation.

4.1.3. Comparison of percentiles

Corresponding with the highest shipping density, the highest median (P50), P05 and P95 -SPLs in the low frequency band (D1, 25–160 Hz)
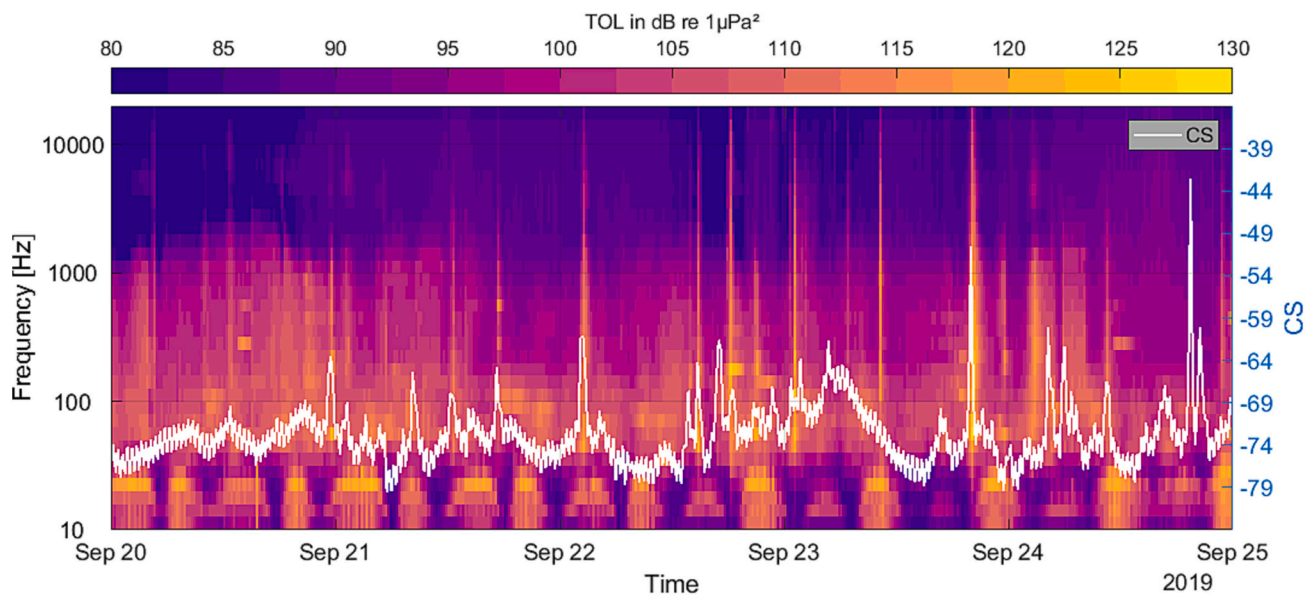
Fig. 4. Spectrogram of measurements at 07-NL-TEX and synchronized distance weighted metric for shipping CS (white line) (see 3.2.2).

were measured at the 08-BE-WST station (114, 124 and 135 dB respectively – see Fig. 7).

The lowest median SPLs in D1 were recorded at the Scottish 11-SC-HEL and the Swedish 01b-SE-HON station (88 and 89 dB respectively). The D1 SPLs at 06-DE-FN1, 07-NL-TEX, 09-UK-DOW and 18-DK-EDA were comparably high. Notably the range between P05 and P95 levels was greatest in the D1 band for many stations (01-SE-VIN, 01b-SE-HON, 02-DK-ANH, 03-DK-HRF, 10-SC-ARB, 16-DK-TN1 and 17-DK-TN4). This variability indicated that transient acoustic events (e.g. ship passages, seismic surveys or construction work) had the highest amplitudes at low frequencies at these stations. P95 levels could also be increased by current noise or platform self-noise. Another source of high variability is low ambient levels between transient events. For example, P05 levels at 01b-SE-VIN, 02-DK-ANH, 10-SC-ARB and 11-SC-HEL are significantly lower than at other stations.

In the D2 frequency band (0.2–1.6 kHz), less variation across the stations and across the percentiles was visible than in the D1 frequency band. Stations 06-DE-FN1 and 18-DK-EDA showed highest median SPL (117 and 123 dB re 1 μPa respectively) in this frequency range. Both stations are close to industrial structures (Offshore Wind Farms and Oil rigs), while stations close to shipping lanes (09-UK-DOW, 15-SC-CNS, 08-BE-WST, 16-DK-TN1 and 17-DK-TN4) also had high SPLs (107 < P50 < 114 dB re 1 μPa).

In the high broadband (D3, 2–10 kHz), the station 18-DK-EDA had the highest SPL across all percentiles (109, 118 and 124 dB respectively). The median levels of the other stations are relatively close to each other and the variability between P05 and P95 percentile is lowest in this band. Several stations (04-DE-FN3, 06-DE-FN1, 08-BE-WST, 09-UK-DOW, 10-SC-ARB, 12-SC-MOR and 16-DK-TN1) also had high P95 SPLs at high and mid frequencies, however it is uncertain what caused these relatively high-amplitude high-frequency noise periods.

4.1.4. Clustering

The results of the pairwise two-sample Kolmogorov-Smirnov test between the 18 stations can be seen in the Fig. 8 for all three broadbands (D1-D3). The resulting clusters are plotted as dendrograms in the left column and geographically distributed in the right column, with each colour representing one cluster. The results of all pairwise comparisons are provided in the supplementary Fig. F. Stations belonging to the same cluster are assumed to record similar ambient noise in the respective frequency bands.

Four clusters were identified for the D1 band, reflecting the influence of flow noise. As such these clusters not only collate stations of similar sound pressure levels, but also stations of similar current velocities. The blue cluster comprises the stations with highest received levels in this frequency band (see Fig. 8) and - with exception of the 18-DK-EDA station - also the stations with highest current velocities (06-DE-FN1, 07-NL-TEX and 08-BE-WST with maximum current velocities equal or >0.56 m/s), which are thus the most susceptible to flow noise. Station 18-DK-EDA is assumed to be rather affected by noise of the adjacent oil rig and not by high flow noise. Sound pressure levels at stations from the orange cluster are slightly lower - especially for the 5 % percentile - indicating that the main difference to the blue cluster is a quieter ambient background. The purple cluster comprises the quietest stations at this frequency range, where the 5 % percentile is below 85 dB and maximum current velocities are relatively low (below 0.23 m/s). This distinction based on current velocity is not valid for all stations, for example, the current speeds are generally low at the 14-NO-NTR station. Flow noise mainly affects frequencies up to 63 Hz (see Section 4.2.3); therefore, current velocities are not likely to explain all patterns found in D1 (up to 160 Hz).

Stations generally sort into two main clusters in the D2 frequency band. Stations belonging to the light blue cluster are characterised by higher sound pressure levels. In contrast to the green cluster all stations of the light blue cluster have 5 % percentile levels above 100 dB. The intermittent sound pressure levels (95 % percentile levels) are distinctively higher in the light blue cluster, where all P95 levels are above 116 dB. The distribution of the clusters can be roughly explained by the presence of shipping around the stations where stations with high shipping (e.g.06-DE-FN1, 07-NL-TEX and 08-BE-WST) belong to the light blue clusters with relatively high sound pressure levels and stations with less traffic (e.g. 1b-SE-VIN, 03-DE-FN3 or 14-NO-NTR) belong to the quieter green cluster.

Station 18-DK-EDA belongs to no cluster in either the D2 or the D3 band and seems to be distinct from and louder than the adjacent 05-DE-ES1 station (P05 of 109 dB in D3). This indicates that the mid- and high frequency bands of this station are dominated by other sound sources, probably due to the adjacent oil rig.

Most stations belonged to the blue cluster in the D3 band. In general, the differences between the stations (Euclidean distances) are smaller in the D3 band compared to other frequency bands. This confirms that wind affects most parts of the North Sea in the high frequency bands uniformly. The stations that do not belong to the blue cluster are either located in relatively deep waters (10-SC-ARB, 11-SC-HEL, 12-SC-MOR
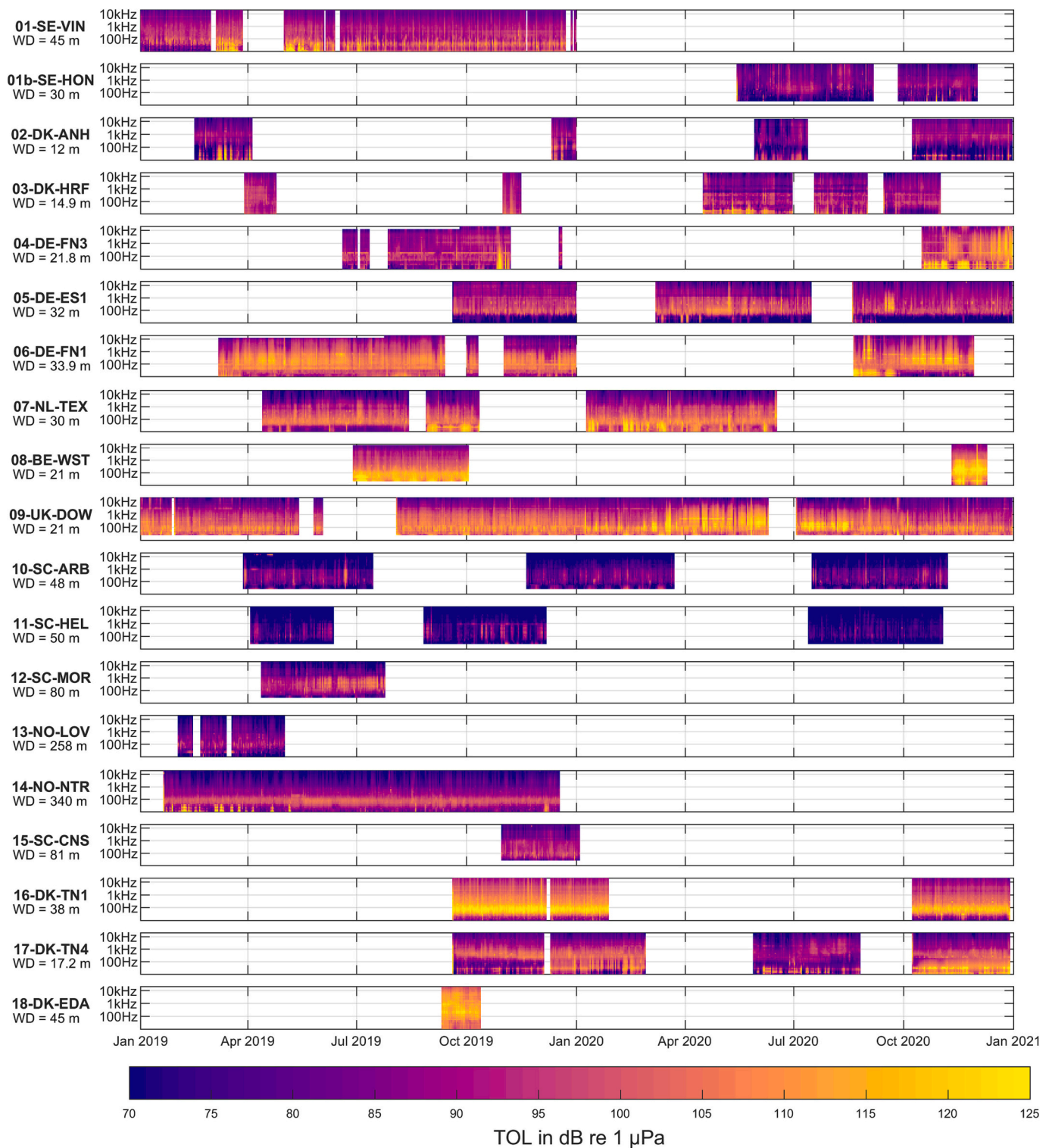
Fig. 5. Spectrograms of one-third octave levels for all measurements from 2019 and 2020 at all 19 JOMOPANS stations; water depths (WD) are given for each station.

and 14-NO-NTR) or, in the case of the 01b-SE-HON station, protected from wind by nearby islands.

It is noteworthy that some stations belong to similar clusters across all frequency bands. As such we can identify a distinct cluster of similar stations in the south, comprising the heavily trafficked stations 06-DE-FN1, 07-NL-TEX and 08-BE-WST. The Scottish coastal stations 10-SC-ARB and 11-SC-HEL form a second persistent cluster.

4.2. Correlation with wind, shipping and currents

Spearman correlation coefficients for all stations with wind, shipping and currents are displayed in Fig. 9. Fig. 10 illustrates the linear scaling factors for wind speeds and current velocities. These factors can be used as a tool to estimate sound levels in areas where measurements are not available. They quantify the linear relationships between received sound pressure levels and the logarithm of wind speed and the relationship
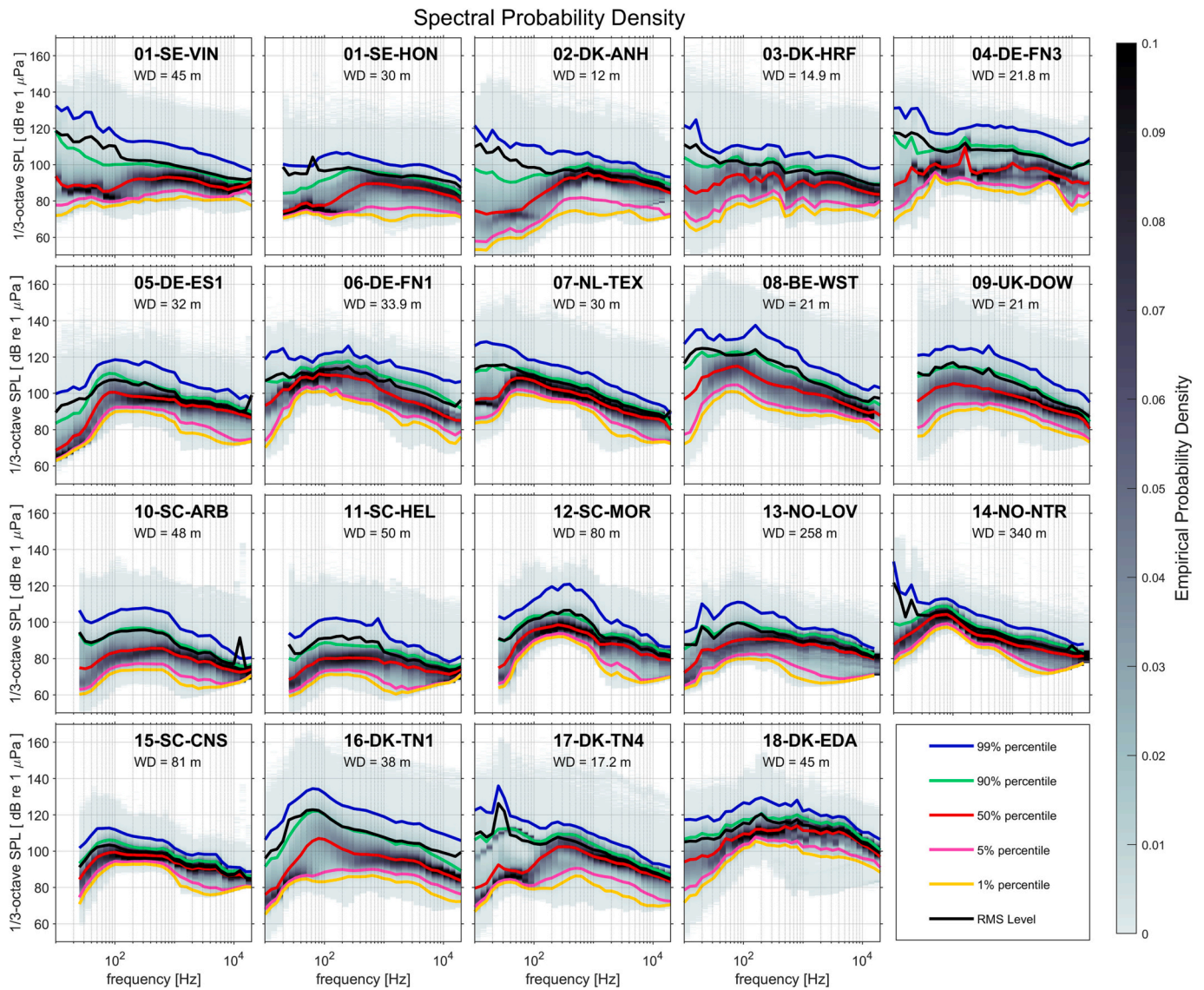
Spectral Probability Density

Fig. 6. Spectral Probability Densities for all measurements (2019 and 2020) overlaid with cumulative probability distributions of the 1 %, 5 %, 50 %, 90 % and 99 % percentiles as well as RMS levels for all TOLs; water depths (WD) are given for each station.
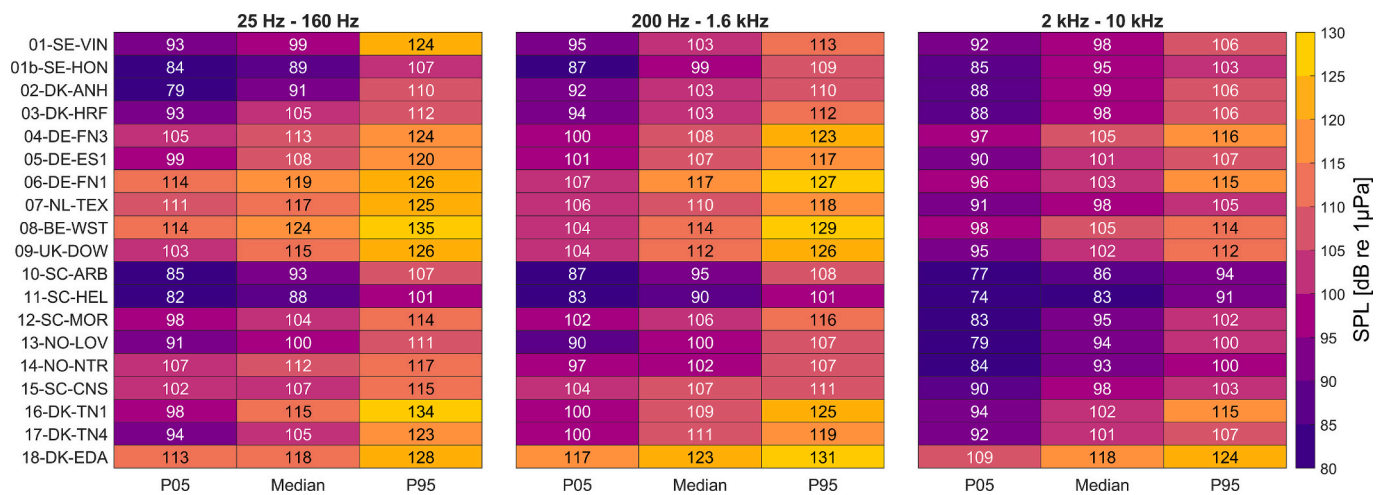

Fig. 7. 5 % percentile, median and 95 % percentile of broadband sound pressure levels at all measurement stations (for 2019 and 2020) for D1 (left), D2 (centre) and D3 (right);
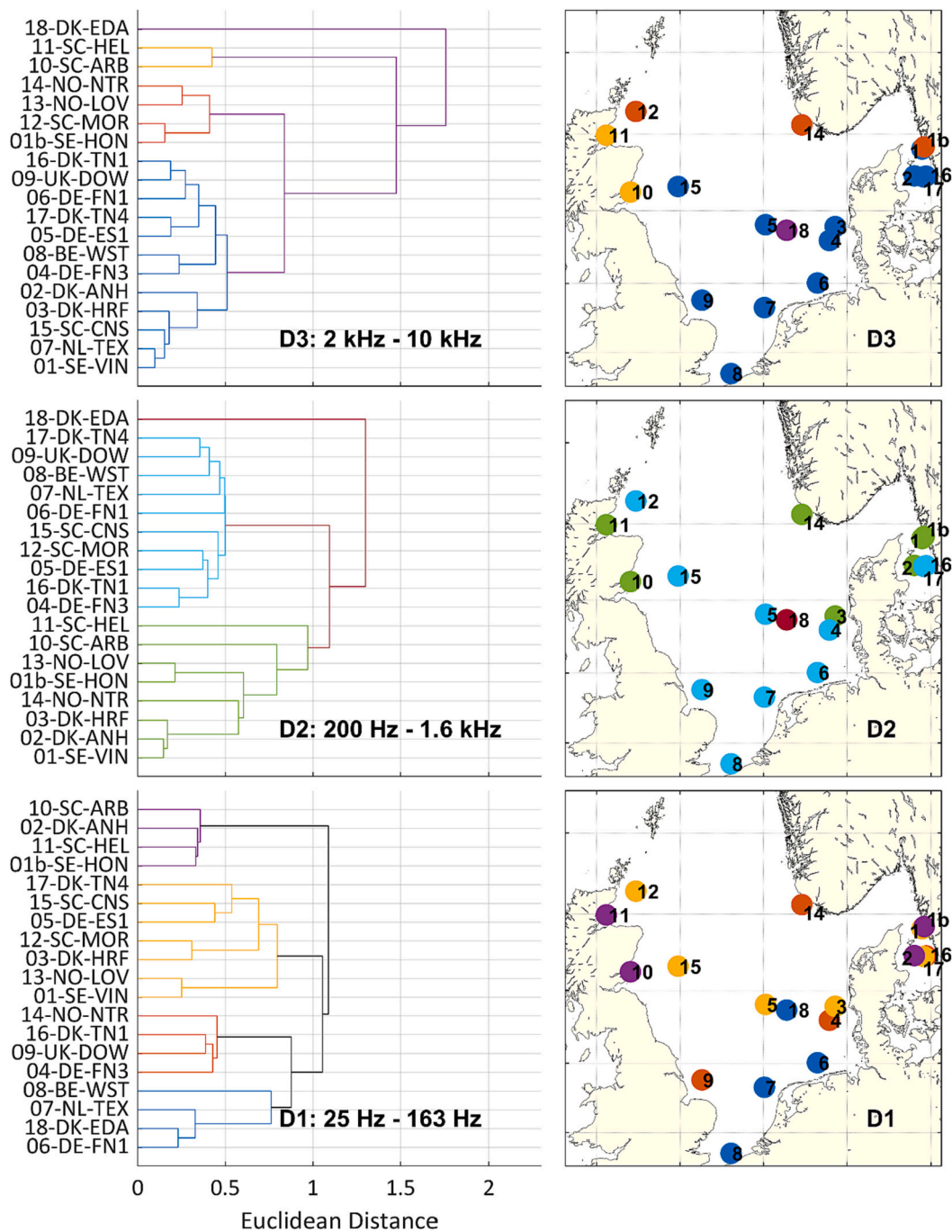
Fig. 8. Dendrograms calculated for Euclidean distances to form clusters from KS-test-statistic-matrix for each decadal band (left) – geographical representation of clusters (right) – same colours indicate that stations belong to the same cluster; note that 13-NO-LOV is outside of the shown map; all data from 2019 and 2020 were considered in this comparison.

between flow noise and the logarithm of current speed for the observed stations in the North Sea.

No wind-, shipping and current data were available for the 13-NO-LOV station, which was therefore excluded from these comparisons. A comparison between ocean currents, shipping and wind in the low frequencies (down to 10 Hz) and high frequencies (up to 20 kHz) was not possible at all stations (e.g. Belgium, England, Germany, Scotland and Norway stations) due to equipment limitations. Positive as well as negative correlations could be observed and will be discussed in the following.

4.2.1. Correlation with wind speed

The mean modelled wind speeds at the stations were relatively uniform (Table 2), indicating that the wind effect is evenly distributed across the stations. This assumption is supported by the model results of the JOMOPANS project, which also found that wind noise varies only little over the North Sea area (de Jong et al., 2021), and by the large clusters for D3 (see Fig. 8).

As expected, for TOLs above 500 Hz, high positive correlations with wind speed are observed at almost all stations. These correlations also represent the highest correlations we could identify in the data sets, up to 0.9, suggesting that wind-induced noise strongly influences the high-frequency ambient noise around the North Sea. The measured sound
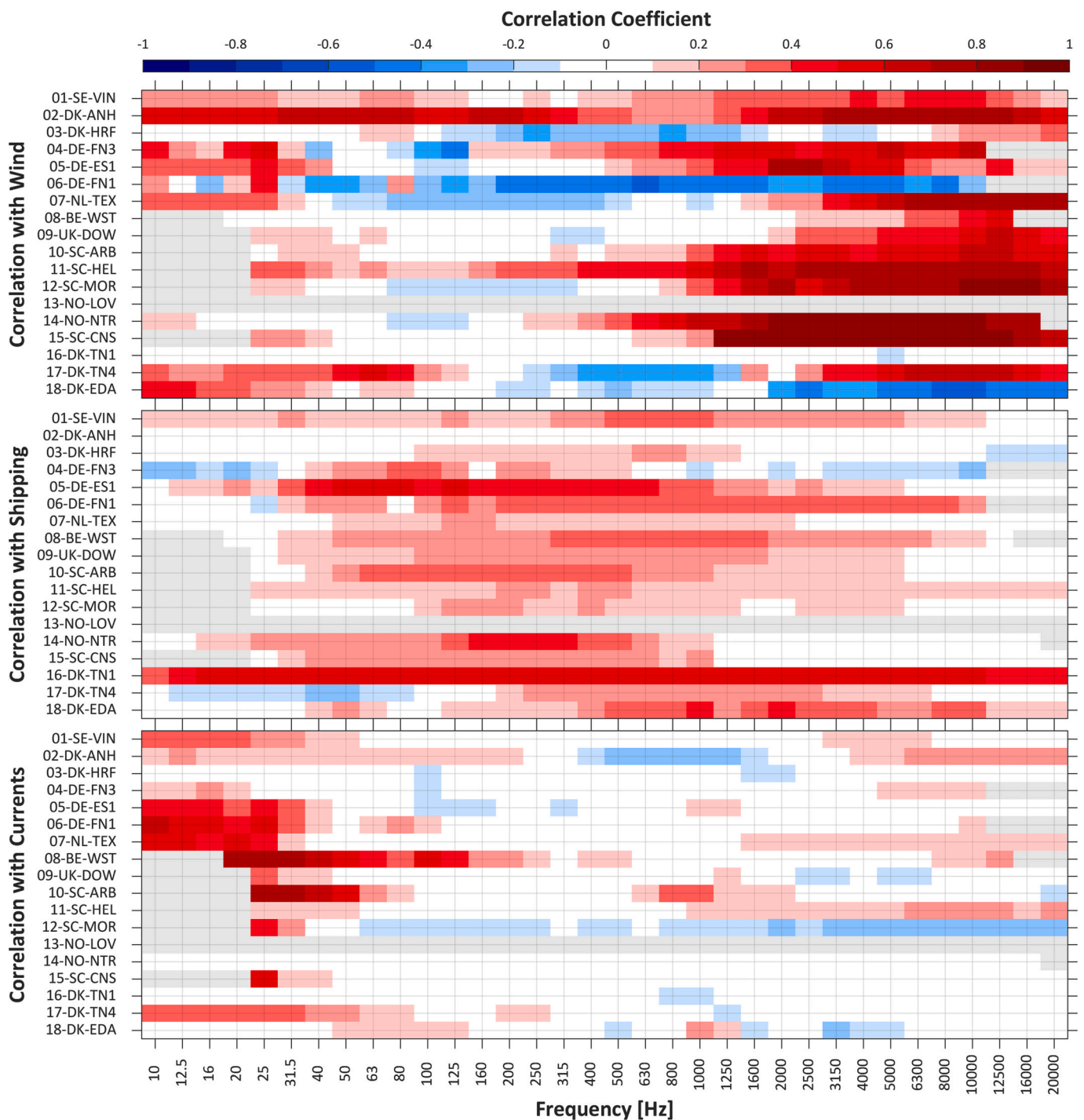
Fig. 9. Spearman Correlation Coefficients for wind, shipping and currents for each TOL and for respective noise sources; see 3.2.2 for derivation of distance-weighted shipping metric CS which was used for correlations with shipping; Non-available one-third octave bands are displayed in grey; no wind, shipping and current data were available for 13-NO-LOV; all correlations are based on the data from 2019.

pressure levels scale with 10 to 30 times the base 10 logarithm of the wind speed in the high frequency bands. This is well in line with results from previous studies that found similar factors in measured data (e.g. Chapman and Cornish, 1993; Cato and Tavener, 1997; Reeder et al., 2011) as well as with semi-empirical models that suggest that the scaling factor should be 22.4 (de Jong et al., 2021; Ainslie, 2010). Although we observe some scatter around reported values, we can confirm scaling laws of similar magnitude for frequency bands with high correlation. In the literature, higher factors (~30) have been measured where wind-dependent noise has been largely isolated from other sources and

lower values result where there is significant contribution from other sources of noise. The presence of shipping noise at frequencies between 63 Hz and 2 kHz (see Fig. 9) thus supports the relatively low scaling factors with wind in this frequency range.

Wind speeds are also positively correlated with low frequency TOLs at most stations, although generally at lower amplitudes, possibly due to wind-driven currents and thus flow noise (see Fig. 11). The scaling law shows that with increasing wind speed, the sound pressure levels at low frequencies increase with a scaling factor up to 40 (at 02-DK-ANH, 04-DE-FN3 and 07-NL-TEX).
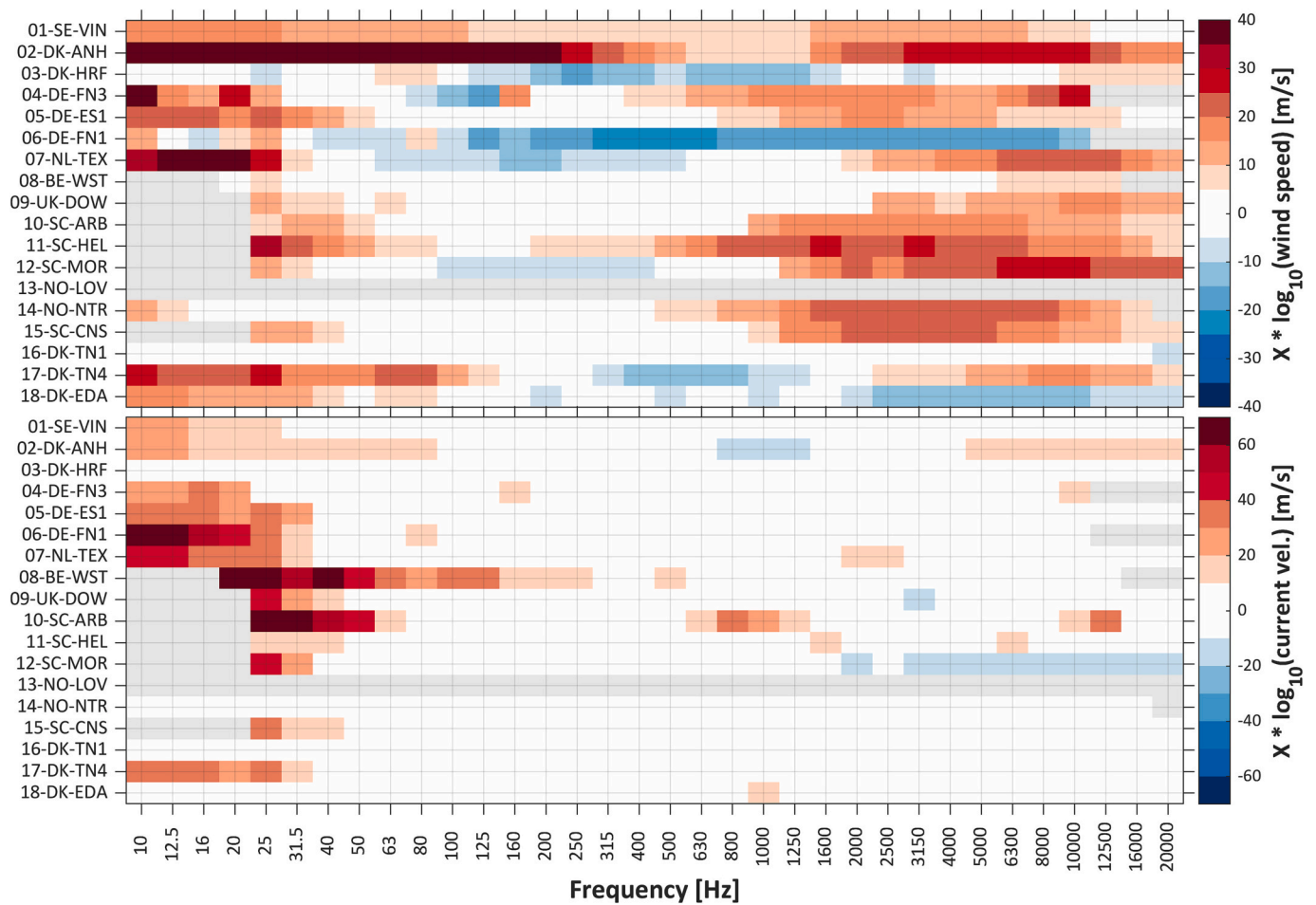
Fig. 10. Scaling factors "X" for wind speed and current velocities for each TOL; Non-available one-third octave bands are displayed in grey; no wind and current data were available for 13-NO-LOV; all results are based on the data from 2019.

In addition to positive correlations, negative correlations with wind speed can also be observed, indicating decreasing TOLs with increasing wind speed, at mid-frequencies (e.g. at 03-DK-HRF or 07-NL-TEX). For 06-DE-FIN and 18-DK-EDA the negative correlations even reach the high frequency bands. An increase in wind speed (and therefore sea state) is generally correlated with less shipping activity (see Fig. 11), which may explain the decrease in TOLs at mid-frequencies. The higher propagation loss of shipping noise due to a rougher sea state could contribute to this effect.

4.2.2. Correlation with shipping

Shipping correlates with TOLs over much of the frequency range recorded. For most stations, the correlation is centred in the frequency range from about 63 Hz to 2 kHz. At some stations weak to moderate (0.2–0.6) correlations were also identified at high frequencies above 4 kHz (01-SE-VIN, 06-DE-FN1, 08-BE-WST, 11-SC-HEL, 16-DK-TN1 and 18-DK-EDA). This could be due to vessels operating closer to the hydrophones (e.g. at the coastal stations 01-SE-VIN, 11-SC-HEL or 16-DK-TN1) or due to vessels that regularly produce noise in higher frequency ranges (e.g. by pushing against piles for crew transfers or by operating highly cavitating thrusters – i.e. during Dynamic Positioning). The latter could be relevant for stations close to wind farms (06-DE-FN1, 08-BE-WST) or oil rigs (18-DK-EDA).

At 01-SE-VIN and at 16-DK-TN1 most or even the whole frequency range is positively correlated with shipping.

Correlations range up to strong correlations (> 0.6) at 05-DE-ES1 and 16-DK-TN1, but are generally weak to moderate across the stations. The relatively weak correlations can be explained by the

simplified method, which only considers the vessel's distance to the hydrophones, but does not account for varying source levels between ships due to their speed, size orientation. However, the presented method suffices to identify frequency bands that are affected by ship noise.

4.2.3. Correlation with ocean currents

Positive correlation with currents at low frequencies indicates the disturbance of the measurements by flow noise at the respective measurement positions. Stations with strongest tidal influence, such as 06-DE-FN1, 07-NL-TEX, 08-BE-WST, 09-UK-DOW showed strong correlations up to 40 Hz (weak correlations up to 500 Hz at 08-BE-WST). This is in line with the highest modelled bottom currents (Table 2). The tidal effect and thus the flow noise was lower at other stations (01-SE-VIN, 02-DK-ANH, 11-SC-HELand 14-NO-NTR) or not detectable at all (03-DK-HRF, 04-DE-FN3 and 05-DE-ES1).

It also needs to be noted, that the deeper 16-DK-TN1 station in contrast to the adjacent 17-DK-TN4 only showed very weak correlation with currents in the 10 Hz one-third octave band, indicating local variability in flow noise due to the bathymetry.

The TOLs for frequencies of high correlation show high scaling factors with the base 10 logarithm of the current velocities - confirming a linear scaling law between the two variables. The scaling factor at which TOLs increase with increasing flow speeds ranges from ~30 e.g. at 07-NL-TEX, 08-BE-WST and 09-UK-DOW to ~60 at 02-DK-ANH. From experiments, Abshagen (2009a, 2009b) reports of scaling factors of about 60. However, hydrophones measurements in the North Sea may differ substantially from these results due to high variability and also
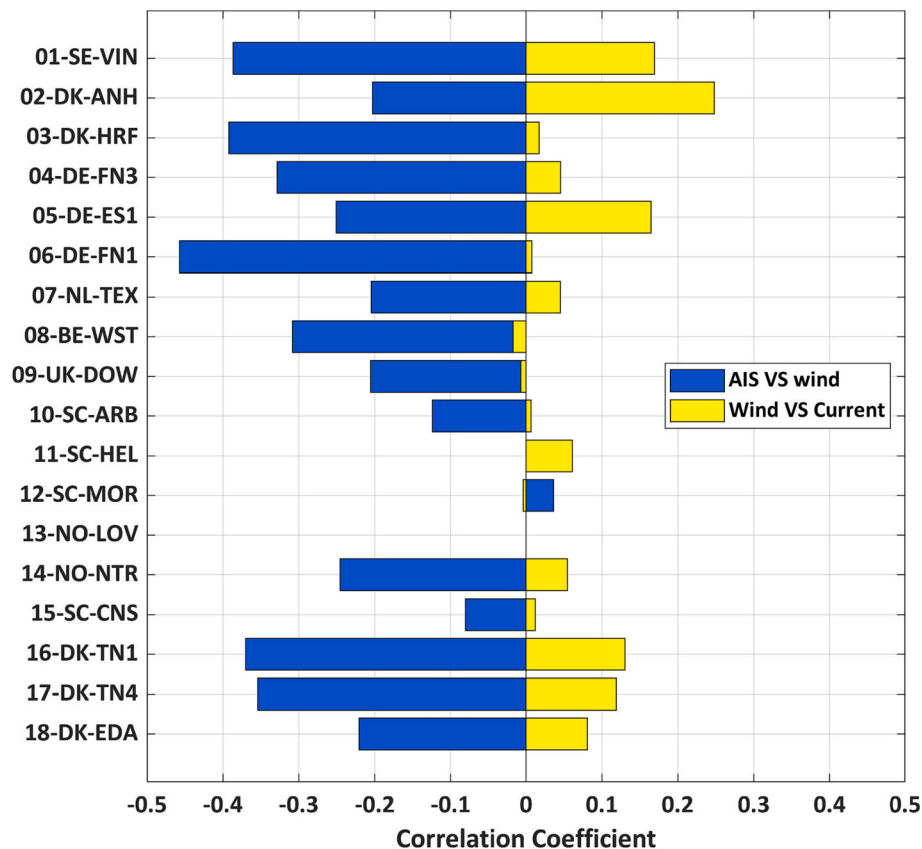
Fig. 11. Spearman correlation coefficients of AIS counts (for a radius of 35 km) and modelled wind (blue) and modelled wind and modelled currents (yellow) for each JOMOPANS station. (For interpretation of the references to colour in this figure legend, the reader is referred to the web version of this article.)

complexity of flow noise. Vortex shedding and cable vibration may have influenced the scaling factors as well as other contributions to the SPL in addition to flow noise.

Table 3 summarises the one-third octave bands of highest correlation and the corresponding scaling factors for wind and flow.

5. Discussion & conclusion

This international study offered unprecedented insight into the North Sea soundscape over a wide spatial and temporal scale. The temporal variability of SPLs at individual stations was found to be higher at shallow stations in the southern North Sea whereas more persistent SPLs were measured at the deeper northern stations. Propagation loss in shallower waters is greater than in deeper waters (for frequencies where ship noise dominates, <1–2 kHz). The higher number of vessels operating in the southern North Sea combined with increased transmission losses thus results in higher variability of received sound levels. In deeper water however, sound travels further and ships from a greater distance contribute to received sound levels. Individual ship passages then tend to average out. Depth also determines which frequencies propagate best under water (Jensen and Kuper, 1983). The dominant frequencies are lower at the deep stations in Norway (13-NO-LOV and 14-NO-NTR) than at the shallower stations in the southern North Sea. At most stations the depths are <50 m and therefore the optimal frequencies that propagate the furthest are expected to be between 500 and 1000 Hz, which coincides with the frequency range of maximum ship noise energy. At very shallow stations we can also observe cut-off effects, where low frequencies below 100 Hz do not seem to propagate at all (e. g. at 02-DK-ANH).

The temporal variability was relatively low compared to the spatial variability of SPLs across the different stations. SPLs were also higher in

the shallower southern North Sea compared to deeper northern stations, consistent with previous model results. A limitation of this study was that fewer stations were operational in the northern North Sea and Norwegian Trench. Therefore, it would be advantageous to increase monitoring efforts in remote areas of the North Sea where validation of soundscape maps has not been possible (Putland et al., 2022).

The highest SPLs at all stations were measured between 100 Hz and 500 Hz. These frequencies are consistent with radiated noise from vessels, which were expected to dominate ambient noise across the North Sea region due to high levels of shipping traffic. Indeed, strong correlations with local shipping density were often observed in the mid-frequency band (50 Hz – 1250 Hz; Spearman coefficients of 0.3–0.7; Fig. 9).

The strongest correlations were with wind at frequencies above 500 Hz (Spearman coefficients >0.8). Flow noise also correlated to measurements in low frequencies up to 500 Hz (Spearman coefficients from 0 to 0.9). Flow noise – which is caused by turbulence around the hydrophone and is not present in the environment – was found to occur at almost all stations, with highest correlations between TOL and current velocity at stations that are greatly impacted by tidal currents (especially 08-BE-WST where highest current velocities occur). It was possible to derive linear scaling laws between the TOLs and the logarithm of wind speed and of current velocities. As these scaling factors were largely consistent between the stations, they provide a simple method of describing the relationship between TOLs and wind speed and contamination from flow noise.

Several statistical tests were carried out to evaluate geographical patterns. The pairwise Kolmogorov-Smirnov test identified similarities between monitoring locations, with geographic clusters per three broadbands revealed. For example, large parts of the North Sea were similarly affected by wind noise, which corresponded to low variability

Table 3

Summary of one-third octave bands of highest correlation and corresponding scaling factor for wind speeds and current velocities for each station;

Station	Wind		Shipping	Flow Noise	
	Frequency of highest correlation	Scaling factor	Frequency of highest correlation	Frequency of highest correlation	Scaling factor
01-SE-VIN	10 kHz	7.3	800 Hz	10 Hz	28
02-DK-ANH	6.3 kHz	28.1	1250 Hz	10 kHz	16
03-DK-HRF	20 kHz	6.9	800 Hz	16 Hz	5
04-DE-FN3	5 kHz	12.1	80 Hz	16 Hz	32
05-DE-ES1	2.5 kHz	15.6	125 Hz	12.5 Hz	37
06-DE-FN1	25 Hz	11.4	1.25 kHz	10 Hz	84
07-NL-TEX	12.5 kHz	22.3	125 Hz	20 Hz	39
08-BE-WST	12.5 kHz	5.8	630 Hz	20 Hz	101
09-UK-DOW	12.5 kHz	16.7	1 kHz	25 Hz	41
10-SC-ARB	12.5 kHz	10.2	125 Hz	25 Hz	86
11-SC-HEL	10 kHz	18.2	500 Hz	12.5 kHz	8
12-SC-MOR	16 kHz	22.9	160 Hz	25 Hz	41
13-NO-LOV	–	–	–	–	–
14-NO-NTR	8 kHz	20.0	250 Hz	12.5 kHz	2
15-SC-CNS	5 kHz	21.4	315 Hz	25 Hz	39
16-DK-TN1	10 Hz	2.4	315 Hz	10 Hz	3
17-DK-TN4	8 kHz	15.7	400 Hz	10 Hz	33
18-DK-EDA	12.5 Hz	15.3	1 kHz	1 kHz	13

in the high D3 band, and one large cluster for the shallower stations and another for the deeper stations. In the mid-frequencies (D2), geographical clusters were found to be related to the volume of shipping, and in the low D1 band, clusters were determined by current-induced flow noise. The defined clusters characterised different soundscapes in the North Sea, providing evidence that may be particularly useful for policy-makers to assess which type of noise dominates certain regions and frequency bands.

Considering the large number of stations, the duration of the measurements and variety of human and biological activity in the North Sea it must be emphasised that the JOMOPANS dataset holds much more information than could be presented in a single study. Further work could explore other sound sources including biological sounds and impulsive sounds such as seismic surveys and pile driving.

This study represents one of the major outcomes of JOMOPANS, one of the largest international joint monitoring programmes for underwater noise pollution to date. For the first time sound levels were recorded across the entire North Sea at 19 measurement positions using standardised methods, establishing a benchmark against which to measure future trends. This achievement demonstrates that regional collaboration is both possible and imperative in order to capture the spatial and temporal characteristics of ambient noise at scales relevant to marine ecosystems.

Supplementary data to this article can be found online at https://doi.org/10.1016/j.marpolbul.2023.115891.

Abbreviations

AIS	Automatic Identification System
BSH	Federal Maritime and Hydrographic Agency (Germany)
CS	"contributing shipping" – distance weighted metric for shipping density (see 3.2.2)
DFT	Discrete Fourier Transform
DP	Dynamic Positioning
ECMWF	European Centre for Medium-Range Weather Forecasts
ERA5	ECMWF Reanalysis v5
EU	European Union
GES	Good Environmental State
GT	Gross Tonnage
JOMOPANS	Joint Monitoring Programme for Ambient Noise in the North Sea
KS	Kolmogorov-Smirnov
MSFD	Marine Strategy Framework Directive
OSPAR	Convention for the Protection of the Marine Environment of the North-East Atlantic
SOLAS	International Convention for the Safety of Life at Sea
SPD	Spectral Power Density
SPL	Sound Pressure Level
TG Noise	Technical Group on Underwater Noise
TNO	Netherlands Organization for Applied Scientific Research
TOL	sound pressure level in one-third octave band
URN	Underwater-Radiated Noise
VMS	Vessel Monitoring System

CRediT authorship contribution statement

F. Basan: Data curation, Formal analysis, Investigation, Methodology, Software, Supervision, Visualization, Writing – original draft, Writing – review & editing. **J.-G. Fischer:** Conceptualization, Data curation, Formal analysis, Funding acquisition, Methodology, Software, Supervision, Visualization, Writing – review & editing. **R. Putland:** Conceptualization, Data curation, Formal analysis, Investigation, Writing – review & editing. **J. Brinkkemper:** Data curation, Formal analysis, Writing – review & editing. **C.A.F. de Jong:** Conceptualization, Formal analysis, Funding acquisition, Methodology, Project administration, Software, Writing – review & editing. **B. Binnerts:** Formal analysis, Methodology, Software, Writing – review & editing. **A. Norro:** Data curation, Formal analysis, Funding acquisition, Project administration, Writing – review & editing. **D. Kühnel:** Data curation, Formal analysis, Project administration, Writing – review & editing. **L.-A. Ødegaard:** Data curation, Formal analysis, Writing – review & editing. **M. Andersson:** Data curation, Formal analysis, Funding acquisition, Project administration, Writing – review & editing. **E. Lalander:** Data curation, Formal analysis, Writing – review & editing. **J. Tougaard:** Data curation, Formal analysis, Funding acquisition, Project administration, Writing – review & editing. **E.T. Griffiths:** Data curation, Formal analysis, Writing – review & editing. **M. Kosecka:** Data curation, Formal analysis, Project administration, Writing – review & editing. **E. Edwards:** Data curation, Formal analysis, Funding acquisition, Project administration, Writing – review & editing. **N.D. Merchant:** Data curation, Formal analysis, Funding acquisition, Project administration, Writing – review & editing. **K. de Jong:** Data curation, Formal analysis, Writing – review & editing. **S. Robinson:** Funding acquisition, Methodology, Project administration, Writing – review & editing. **L. Wang:** Writing – review & editing. **N. Kinneging:** Funding acquisition, Project administration, Writing – review & editing.

Declaration of competing interest

The authors declare the following financial interests/personal relationships which may be considered as potential competing interests: Fritjof Basan reports financial support was provided by North Sea

Region of the European Regional Development Fund (InterReg) of the European Union.

Data availability

Processed acoustic data for all stations except 16-DK-TN1, 17-DK-TN4 and 18-DK-EDA are available in the continuous underwater noise database hosted by the International Council for the Exploration of the Seas (ICES, 2022). Other data are available on request.

References

Abshagen, J., 2009a. Estimation of underwater flow noise by wave number decomposition. In: NAG/DAGA 2009, Rotterdam.
Abshagen, J., 2009b. Estimation of underwater flow noise by wave number decomposition. In: NAG/DAGA 2009, Rotterdam.
Ainslie, M., de Jong, C., Laws, R., 2014. Practical spreading laws: the snakes and ladders of shallow water weacustics. In: Proc. 2nd International Conference and Exhibition on Underwater Acoustics, pp. 22–27 (Rhodes, Greece).
Ainslie, M., 2010. Principles of Sonar Performance Modelling. Springer, Berlin Heidelberg.
Ainslie, M., Andrew, R.K., Howe, B.M., Mercer, J.A., 2021. Temperature-driven seasonal and longer term changes in spatially averaged deep ocean ambient sound at frequencies 63–125 Hz. J. Acoust. Soc. Am. 149 (4), 2531–2545. https://doi.org/10.1121/10.0003960.
ANSI, 2009. ANSI S1. 11-2004. American National Standards Institute.
Au, W., Green, M., 2000. Acoustic interaction of humpback whales and whale-watching boats. Mar. Environ. Res. 49 (5), 469–481. https://doi.org/10.1016/S0141-1136(99)00086-0.
Banner, M.L., Cato, D.H., 1988. Physical mechanisms of noise generation by breaking waves — a laboratory study. In: Kerman, B.R. (Ed.), Sea Surface Sound: Natural Mechanisms of Surface Generated Noise in the Ocean. Springer, Netherlands, Dordrecht, pp. 429–436. https://doi.org/10.1007/978-94-009-3017-9_31.
Bonaduce, A., Staneva, J., Behrens, A., Bidlot, J., Wilcke, R., 2019. Wave climate change in the North Sea and Baltic Sea. J. Mar. Sci. Eng. 7, 166. https://doi.org/10.3390/jmse7060166.
Borsani, J., Andersson .M.,.A.,.A.,.A., M., Bou, M., Castellote, M., Weilgart, L., 2023. Setting EU Threshold Values for continuous underwater sound. In: Technical Group on Underwater Noise (TG NOISE). Luxembourg: Jean-Noel Duon, Georg Hanke and Maud Casier. https://doi.org/10.2760/690123,JRC133476.
Brüning, T., Li, X., Schwichtenberg, F., Lorkowski, I., 2021. An operational, assimilative model system for hydrodynamic and biogeochemical applications for German coastal waters. In: Hydrographische Nachrichten, 118 (Rostock: Deutsche Hydrographische Gesellschaft e.V), pp. 6–15. https://doi.org/10.23784/HN118-01.
Cato, D.H., Tavener, S., 1997. Ambient sea noise dependence on local, regional and geostrophic wind speeds: implications for forecasting noise. Appl. Acoust. 51 (3), 317–338. https://doi.org/10.1016/S0003-682X(97)00001-7.
Chapman, N., Cornish, J., 1993. Wind dependence of deep ocean ambient noise at low frequencies. J. Acoust. Soc. Am. 93 (2), 782–789. https://doi.org/10.1121/1.405440.
Dekeling, R.P., Tasker, M.L., Van der Graaf, S., Ainslie, M., Andersson, M., André, M., Young, J.V., 2014. Monitoring Guidance for Underwater Noise in European Seas.
Duarte, C., Chapuis, L., Collin, S., Costa, D., Devassy, R., Eguíluz, V., Juanes, F., 2021. The soundscape of the Anthropocene ocean. Science 371 (6529), eaba4658. https://doi.org/10.1126/science.aba4658.
EMODnet, 2023. European Marine Observation and Data Network (EMODnet) - Human Activities. Retrieved 11 15, 2023, from. https://emodnet.ec.europa.eu/en/human-activities.
European Commission, 2008. Directive 2008/56/EC of the European parliament and of the council establishing a framework for community action in the field of marine environmental policy (Marine Strategy Framework Directive). Off. J. Eur. Union L164, 19–40.
Fischer, R., 2000. Bow Thruster Induced Noise and Vibration. Conference: Dynamic Positioning Committee, Marine Technology Society.
Fischer, J.-G., Kühnel, D., Basan, F., 2021. JOMOPANS measurement guidelines. In: Report of the EU INTERREG Joint Monitoring Programme for Ambient Noise North Sea (JOMOPANS).

Frankish, C.K., von Benda-Beckmann, A.M., Teilmann, J., Tougaard, J., Dietz, R., Sveegaard, S., Nabe-Nielsen, J., 2023. Ship noise causes tagged harbour porpoises to change direction or dive deeper. Mar. Pollut. Bull. 197, 115755 https://doi.org/10.1016/j.marpolbul.2023.115755.
Frisk, G.V., 2012. Noiseonomics: the relationship between ambient noise levels in the sea and global economic trends. Sci. Rep. 2 (437), 2045–2322. https://doi.org/10.1038/srep00437.
van Geel, N.C., Merchant, N.D., Culloch, R.M., Edwards, E.W., Davies, I.M., O'Hara Murray, R.B., Brookes, K.L., 2020. Exclusion of tidal influence on ambient sound measurements. J. Acoust. Soc. Am. 148, 701–714. https://doi.org/10.1121/10.0001704.
Haver, S., Gedamke, J., Hatch, L., Dziak, B., Van Parijs, S., McKenna, M., Mellinger, D., 2018. Monitoring long-term soundscape trends in U.S. waters: the NOAA/NPS Ocean Noise Reference Station Network. Mar. Policy 90, 6–13. https://doi.org/10.1016/j.marpol.2018.01.023.
Hermannsen, L., Beedholm, K., Tougaard, J., Madsen, P.T., 2014. High frequency components of ship noise in shallow water with a discussion of implications for harbor porpoises (Phocoena phocoena). J. Acoust. Soc. Am. 136 (4), 1640–1653. https://doi.org/10.1121/1.4893908.
Hermannsen, L., Mikkelsen, L., Tougaard, J., Beedholm, K., Johnson, M., Madsen, P., 2019. Recreational vessels without Automatic Identification System (AIS) dominate anthropogenic noise contributions to a shallow water soundscape. Sci. Rep. 9 (15477), 15477. https://doi.org/10.1038/s41598-019-51222-9.
Hersbach, H., Bell, B., Berrisford, P., Biavati, G., Horányi, A., Muñoz Sabater, J., Thépaut, J.-N., 2018. ERA5 hourly data on single levels from 1959 to present. In: Copernicus Climate Change Service (C3S) Climate Data Store (CDS), (Accessed on 17-Aug-2022). https://doi.org/10.24381/cds.adbb2d47.
Hildebrand, J., 2009. Anthropogenic and natural sources of ambient noise in the ocean. In: Marine Ecology-progress Series-MAR ECOL-PROGR SER, vol. 395, pp. 5–20. https://doi.org/10.3354/meps08353.
Hildebrand, J.A., Frasier, K.E., Baumann-Pickering, S., Wiggins, S.M., 2021. An empirical model for wind-generated ocean noise. J. Acoust. Soc. Am. 149 (6), 4516. https://doi.org/10.1121/10.0005430.
Holthuijsen, L., 2007. Waves in Oceanic and Coastal Waters. Waves in Oceanic and Coastal Waters, by Leo H. Holthuijsen, pp. 404. Cambridge University Press, January 2007. ISBN-10. ISBN-13. https://doi.org/10.2277/0521860288.
ICES, 2022. Continuous Noise Database. Retrieved from. https://underwaternoise.ices.dk/continuous.
IEC. (n.d.). 61260-1:2014.
ISO. (n.d.). 18405:2017.
Jensen, F.B., Kuper, W.A., 1983. The optimum frequency of propagation in shallow-water environments. J. Acoust. Soc. Am. 73 (3), 813–819. https://doi.org/10.1121/1.389049.
Jomopans-Interreg North Sea Region, 2021. Retrieved 8 17, 2022, From Jomopans GES Tool. https://jomopansgestool.au.dk/en/.
de Jong, C., Binnerts, B., Robinson, S., Wang, L., 2021. Guidelines for modelling ocean ambient noise. In: Report of the EU INTERREG Joint Monitoring Programme for Ambient Noise North Sea (Jomopans).
de Jong, C., Binnerts, B., de Krom, P., Gaida, T., 2022. North Sea Sound Maps 2019-2020. Report of the EU INTERREG Joint Monitoring Programme for Ambient Noise North Sea (Jomopans).
Kinneging, N., Andersson, M.H., Robinson, S., De Jong, C., Fischer, J., Merchant, N., Tougaard, J., 2021. 10 years of North Sea soundscape monitoring. In: Looking Back on a Four-year Interreg NSR Project and Looking Forward to the Six-year Monitoring Cycle. Retrieved from. https://northsearegion.eu.
Kinneging, N., Andersson, M.H., De Jong, C., De Jong, K., Fischer, J., Kosecka, M., Tougaard, J., 2023. Joint Monitoring Programme for Ambient Noise in the North Sea. In S. J. Popper, A.N., The Effects of Noise of Aquaric Life. Springer. https://doi.org/10.1007/978-3-031-10417-6 79-1.
Knudsen, V.O., Alford, R.S., Emling, J.W., 1948. Underwater ambient noise. J. Mar. Res. 7 (3), 410–429.
Lalander, E., Nordström, R.L., Andersson, M.H., 2022. Changes in the underwater soundscape in Kattegat due to shipping re-routing. FOI-R–5334–SE, ISSN 1650-1942. Retrieved from. https://www.foi.se/en/foi/reports/report-summary.html?reportNo=FOI-R–5334-SE.
Li, S., Li, M., Gerbi, G.P., Song, J., 2013. Roles of breaking waves and Langmuir circulation in the surface boundary layer of a coastal ocean. J. Geophys. Res. Oceans 118 (10), 5173–5187. https://doi.org/10.1002/jgrc.20387.
Medwin, H., Beaky, M.M., 1989. Bubble sources of the Knudsen sea noise spectra. J. Acoust. Soc. Am. 86 (3), 1124–1130. https://doi.org/10.1121/1.39810 4.
Merchant, N.D., Blondel, P., Dakin, D.T., Dorocicz, J., 2012. Averaging underwater noise levels for environmental assessment of shipping. J. Acoust. Soc. Am. 132 (4), EL343-EL349 https://doi.org/10.1121/1.4754429.
Merchant, N., Barton, T., Thompson, P., Pirotta, E., Dakin, T., Dorocicz, J., 2013. Spectral probability density as a tool for ambient noise analysis. J. Acoust. Soc. Am. 133 (4), EL262-EL267 https://doi.org/10.1121/1.4794934.
Merchant, N., Farcas, A., Powell, C., 2018. Acoustic metric specification. In: Report of the EU INTERREG Joint Monitoring Programme for Ambient Noise North Sea (Jomopans).
Merchant, N.D., Putland, R.L., André, M., Baudin, E., Felli, M., Slabbekoorn, H., Dekeling, R., 2022. A decade of underwater noise research in support of the European Marine Strategy Framework Directive. Ocean Coast. Manag. 228 (0964-5691), 106299 https://doi.org/10.1016/j.ocecoaman.2022.106299.
Mustonen, M., Klauson, A., Andersson, A., Clorennec, D., Folegot, T., Koza, R., Sigray, P., 2019. Spatial and temporal variability of ambient underwater sound in the Baltic Sea. Sci. Rep. 9, 1–13. https://doi.org/10.1038/s41598-019-48891-x.

Ødegaard, L., Pedersen, G., Johnsen, E., 2019. Underwater Noise from Wind at the high North LoVe Ocean Observatory. UACE2019- Conference Proceedings, UACE 2019 (5th Underwater Acoustic Conference and Exhibition), 359-366.

Olmer, N., Comer, B., Roy, B., Mao, X., Rutherford, D., 2017. Greenhouse gas emissions from global shipping, 2013-2015. Retrieved 08 17, 2022, from The International Council on Clean Transport. https://theicct.org/wp-content/uploads/2021/06/Global-shipping-GHG-emissions-2013-2015_ICCT-Report_17102017_vF.pdf.

Putland, R.L., de Jong, C., Binnerts, B., Farcas, A., Merchant, N.D., 2022. Multi-site validation of shipping noise maps using field measurements. Mar. Pollut. Bull. 179, 113733 https://doi.org/10.1016/j.marpolbul.2022.113733.

Reeder, D.B., Sheffield, E.S., Mach, S.M., 2011. Wind-generated ambient noise in a topographically isolated basin: a pre-industrial era proxy. J. Acoust. Soc. Am. 129 (1), 64–73. https://doi.org/10.1121/1.3514379.

Richardson, W.J., Greene, C.R., Malme, C.I., Thomson, D.H., 1995. Marine Mammals and Noise. Academic Press, San Diego, CA. https://doi.org/10.1016/C2009-0-02253-3.

Robinson, S., Wang, L., 2021. Terminology for ocean ambient noise monitoring. In: Report of the EU INTERREG Joint Monitoring Programme for Ambient Noise North Sea (Jomopans).

Robinson, S., Lepper, P., Hazelwood, R., 2014. Good Practice Guide No. 133 Underwater Noise Measurement.

Smirnov, N.V., 1939. Estimating the deviation between the empirical distribution functions of two independent samples. Bulletin de l'Universite de Moscou 2, 3–16.

Snoek, R.C., Ainslie, M.A., Prior, M.K., van Onselen, E., 2015. OSPAR Monitoring Strategy for Ambient Underwater Noise. OSPAR Commission, Agreement 2015-05.

Soulsby, R.L., Smallman, J.V., 1986. A direct method of calculating bottom orbital velocity under waves. In: Hydraulics Research Limited, 76 (14pp).

Spearman, C., 1904. The proof and measurement of association between two things. (JSTOR, Ed.). Am. J. Psychol. 15 (1), 72–101. https://doi.org/10.2307/141 2159.

Sündermann, J., Pohlmann, T., 2011. A brief analysis of North Sea physics. Oceanologia 53 (3), 663–689. https://doi.org/10.5697/oc.53-3.663.

Tattini, J., McBain, S., 2021. International Shipping-Analysis-IEA. Retrieved 8 17, 2022, From International Energy Agency. https://www.iea.org/reports/international-shipping.

Thomsen, F., Erbe, C., Hawkins, A., Lepper, A., Popper, P., Scholik-Schlomer, A.N., Sisneros, J., 2020. Introduction to the special issue on the effects of sound on aquatic life. J. Acoust. Soc. Am. 148 (2), 934–938. https://doi.org/10.1121/10.0001725.

Van der Graaf, A.J., Ainslie, M.A., André, M., Brensing, K., Dalen, J., Dekeling, R., Werner, S., 2012. European Marine Strategy Framework Directive-Good Environmental Status (MSFD GES): Report of the Technical Subgroup on Underwater Noise and Other Forms of Energy.

Van Roy, W., Scheldeman, K., Van Roozendael, B., Van Nieuwenhove, A., Schallier, R., Vigin, L., Maes, F., 2022. Airborne monitoring of compliance to NOx emission regulations from ocean-going vessels in the Belgian North Sea. Atmos. Pollut. Res. 13 (9) https://doi.org/10.1016/j.apr.2022.101518 (1309-1042).

Wang, X.-T., Liu, H., Lv, Z.-F., Deng, F.-Y., Xu, H.-L., Qi, L.-J., He, K.-B., 2021. Trade-linked shipping CO2 emissions. Nat. Clim. Chang. 11, 945–951. https://doi.org/10.1038/s41558-021-01176-6.

Ward, J., Wang, L., Robinson, S., Harris, P., 2021. Standard for Data Processing of Measured Data. Report of the EU INTERREG Joint Monitoring Programme for Ambient Noise North Sea (Jomopans).

Wenz, G.M., 1962. Acoustic ambient noise in the ocean: spectra and sources. J. Acoust. Soc. Am. 34 (12), 1936–1956. https://doi.org/10.1121/1.19 09155.

Wisniewska, D., Johnson, M., Teilmann, J., Siebert, U., Galatius, A., Dietz, R., Madsen, P., 2018. High rates of vessel noise disrupt foraging in wild harbour porpoises (Phocoena phocoena). Proc. R. Soc. B Biol. Sci. 285, 20172314. https://doi.org/10.1098/rspb.2017.2314.